A mining research contract report
APRIL 1983

DEVELOPMENT OF A HYDRIDE FUEL SYSTEM FOR UNDERGROUND MINE USE

Contract H0202034
Eimco Mining Machinery International

OFR
84-79

BUREAU OF MINES
UNITED STATES DEPARTMENT OF THE INTERIOR

DISCLAIMER NOTICE

The views and conclusions contained in this document are those of the authors and should not be interpreted as necessarily representing the official policies or recommendations of the Interior Department's Bureau of Mines or of the U.S, Government.

50272-101

REPORT DOCUMENTATION PAGE	1. REPORT NO.	2.	3. Recipient's Accession No.
4. Title and Subtitle Hydride Fuel System for Underground Mine Use Development and Testing			5. Report Date April 15, 1983 6.
7. Author(s) Ned Baker, Frank Lynch			8. Performing Organization Rept. No. 7405-3
9. Performing Organization Name and Address Eimco Mining Machinery International Salt Lake City, Utah			10. Project/Task/Work Unit No. 11. Contract(C) or Grant(G) No. (C) H0202034 (G)
12. Sponsoring Organization Name and Address U.S. Bureau of Mines Twin Cities Research Center Minneapolis, Minnesota			13. Type of Report & Period Covered Final April 82-April 83 14.

15. Supplementary Notes

16. Abstract (Limit: 200 words)

Details are given of a Hydride Fuel System to provide 5 kg of H_2 to fuel a Caterpillar 3304 engine previously modified to operate on hydrogen fuel and intended to power an underground mining vehicle.

The Fuel System was installed onto the engine and the Engine/Fuel System tested under cold start conditions and a full range of engine loads and speeds. Refueling tests were also performed.

The fuel system tested will support full engine power and allow delivery of at least 3/4-power on a continuous basis, from cold start conditions.

17. Document Analysis a. Descriptors

Underground Mining, Metal/Nonmetal Mines, Mine Safety, Mobile Mining Machinery, Engines, Internal Combustion, Hydrogen, Hydrides, Fuel, Fuel Systems

b. Identifiers/Open-Ended Terms

c. COSATI Field/Group

18. Availability Statement	19. Security Class (This Report)	21. No. of Pages
	20. Security Class (This Page)	22. Price

(See ANSI-Z39.18)

OPTIONAL FORM 272 (4-77)
(Formerly NTIS-35)
Department of Commerce

FOREWORD

This report was prepared by Eimco Mining Machinery International with the assistance of Hydrogen Consultants Inc., under USBM contract H0202034, with Lars Olavson as Program Manager. The contract was initiated under the Metal and Nonmetal Health and Safety Program. It was administered under the technical direction of the Twin Cities Research Center, with Mr. Lito Mejia acting as the Technical Project Officer. Mrs. Sandra Schlesier was the Contract Administrator for the Bureau of Mines.

The report summarizes work completed under this contract from April 1982 through April 15 1983.

ACKNOWLEDGEMENT

Appreciation is expressed to the Technical Project Officer of the U.S. Bureau of Mines, Mr. Lito Mejia for his cooperation, guidance and direct participation in collecting test data.

TABLE OF CONTENTS

LIST OF FIGURES

LIST OF TABLES

INTRODUCTION AND SUMMARY

This study constitutes Phase III of a long-term development program whose objective is a clean, safe and practical energy system for powering underground mining equipment.

The Program phases are:

I. Technical Assessment
II. Engine Development
III. Fuel System Design and Test
IV. Prototype Vehicle Development
V. Surface Demonstration
VI. Underground Demonstration

The time frame for this activity is shown in the bar chart below. The shaded bars are completed phases.

PROGRAM SCHEDULE

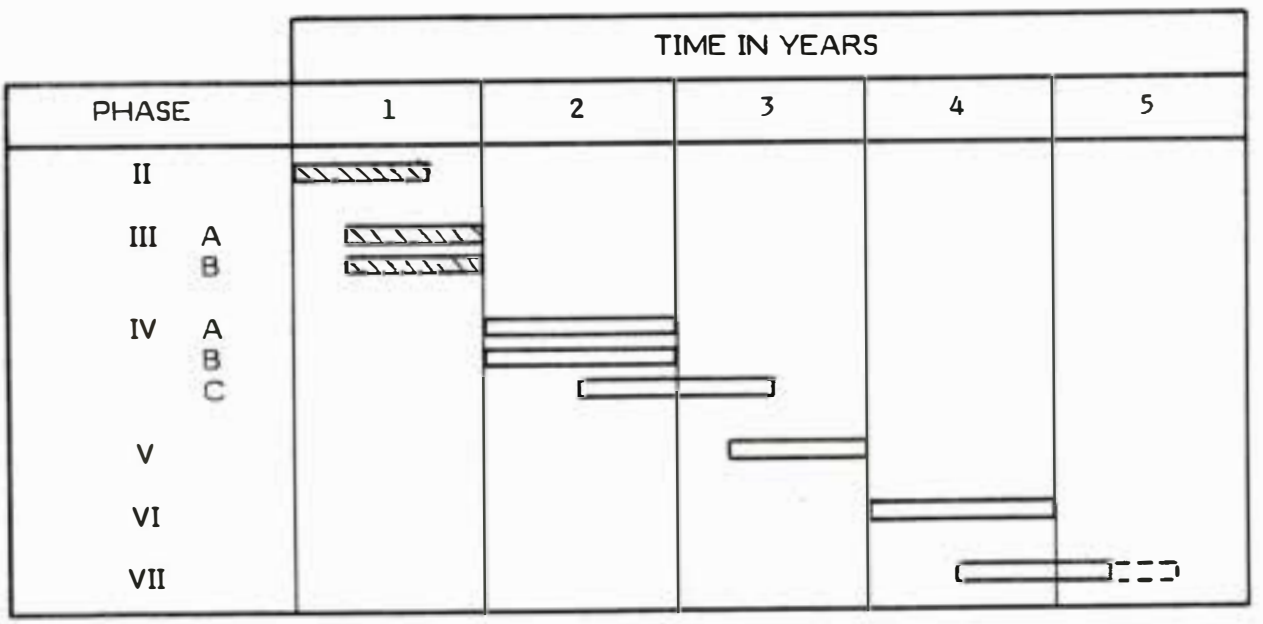

The objectives of the most recent phase of the project were the design, construction and testing of a metal hydride fuel system suitable for supplying the engine developed in Phase II, with 5 Kg of hydrogen fuel.

The project was conducted by Hydrogen Consultants, Incorporated at their facility in Denver, Colorado under a cost-shared arrangement between the U.S. Bureau of Mines and Eimco Mining Machinery International. The hydride alloy used in the fuel system was provided by Ergenics Division of MPD Technology Corp.

The hydride system which has resulted from this phase of the project represents significant advancements in vehicular hydrogen storage methods using metal hydride, solid-state hydrogen containers. The modular design, developed during this phase, is a major step toward a mine-safe hydrogen system which is capable of meeting the safety criteria established in Phase I. A specially designed fuel module, with heat transfer enhancement, demonstrates a means for supplying adequate fuel flow for the hydrogen engine without the high accidental fuel leakage potential of earlier designs.

BACKGROUND

The EIMCO Hydrogen Mining Vehicle Project began in 1977 with the objective of creating an ultra-low emission power system for underground mining machinery. A Caterpillar 3304 pre-chamber diesel was modified for hydrogen fuel and tested in several forms. The engine evolved into a turbocharged, aftercooled, spark-ignition engine with a timed fuel delivery method called Parallel Induction. Figure 1 compares the NOx emissions of the engine, measured during Phase II of this project (1)* with the NOx emissions of two diesel engines commonly used in underground mining. This low-level NOx emission is the only undesirable product of hydrogen combustion. The other emissions of diesels, (smoke, CO, SOx, organics, etc.) are essentially non-existent with hydrogen fuel.

Earlier in the project (1979-1980), a fuel container was built and tested which demonstrated the basic feasibility of using metal hydrides for powering a mining vehicle (2). This prototype hydride container pointed out the severe heat transfer demands and gas flow requirements of a hydride system for a heavy-duty hydrogen engine. The container was grossly overdesigned according to the results of bench-scale modeling experiments (3) but during actual engine tests it was barely sufficient to supply enough fuel flow for some test conditions. The lessons learned during this earlier test program were:

(1) Large liquid capacity of the hydride container's water-jacket caused slow thermal response to heat input from the engine's cooling system.

(2) The use of 2.86 cm (1.125 inch) diameter heat exchanger tubes with a relatively unstable hydride, $(Fe_{0.9}Mn_{0.1})Ti$-H, was barely capable of meeting the demands of the engine during cold-start, high load tests.

(3) The joining methods used to construct the aluminum container were not reliable enough for vehicular service (weld porosity and cracking in mechanical joints).

*Numbers in parenthesis correspond to the references in back of the report.

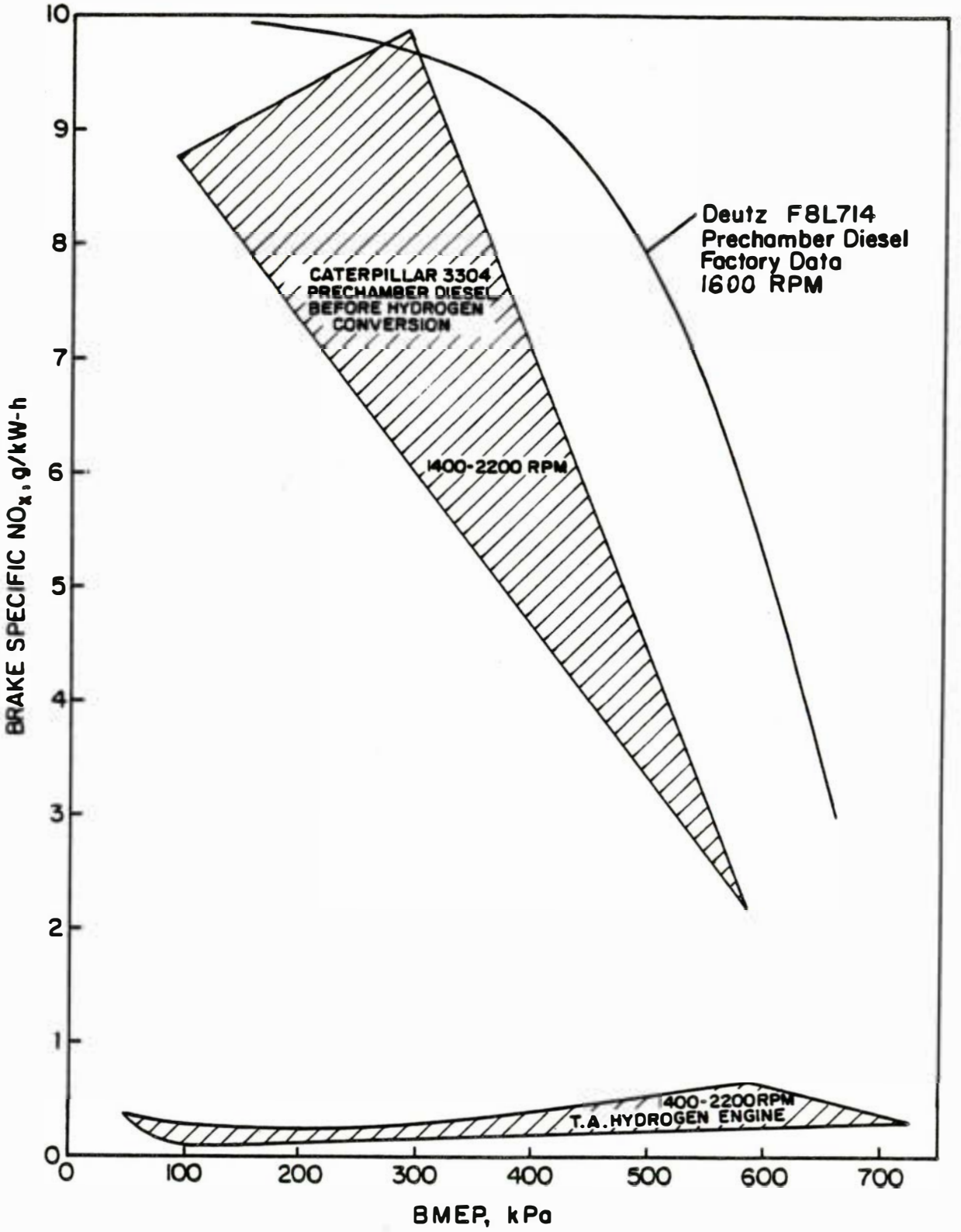

Figure 1. Brake specific oxides of nitrogen vs brake mean effective pressure for the hydrogen fueled Cat 3304 compared to two prechamber diesel engines.

(4) A single, large container is inferior to several smaller ones for many reasons (Thermal response, maintenance problems and difficulty of installation to name a few).

In addition to the experience gained from the early prototype tests, the Technical Assessment Phase of the current program (4) pointed out the difficulty of using conventional metal hydride containers within the safety constraints of underground mining. It became clear that several improvements were needed to make a practical and safe hydride system for underground mining vehicles.

A major criterion for hydrogen safety in underground mines (4) requires that a worst-case accidental rupture of a hydride system will not release enough fuel to cause a safety problem. This safety concept is discussed in some detail in Appendix B. The solution would be as simple as choosing a very low-pressure hydride alloy (many are known) if it were not for the fuel pressure and flow demands of the engine. The project team devised a solution to this apparent dilemma. It was reasoned that a small amount of hydride is safe, no matter what its pressure, since it can release only a small amount of fuel in case of an accident. Several small modules with a very stable hydride alloy could be heated, one at a time, to generate the pressure required by the engine. There are practical difficulties in using a series of small containers with very stable hydrides to fuel a heavy-duty engine. The heat transfer and gas flow capacity of each small hydride module must be increased as its size is decreased relative to a single, large hydride container.

Many efforts to improve the notoriously poor thermal conductivity of hydride powders have been reported in the literature (e.g., 5,6).

CONTAINER DESIGN

If it is assumed that previous tubular container designs will be continued, Fourier's law of heat conduction may be applied in a fairly simple way to show the effects of design changes. Using the previous container's specifications and performance for a starting point, Fourier's law of heat conduction for radial transfer in a cylindrical object,

$$\dot{Q} = \frac{2\pi k L \Delta T}{\ln r_o/r} \quad \text{(Ref. 7)}$$

where:

$\dot{Q}$ = heat flow (and hence hydrogen flow from a hydride)

k = Thermal conductivity

L = Length of tubing

r_o = Outside radius of tubing

r = Radius of the moving reaction front

ΔT = Temperature difference between tubing and reaction

may be used to estimate the effect of design changes on performance. Figure 2 shows the idealized model of hydride containment used for the calculations.

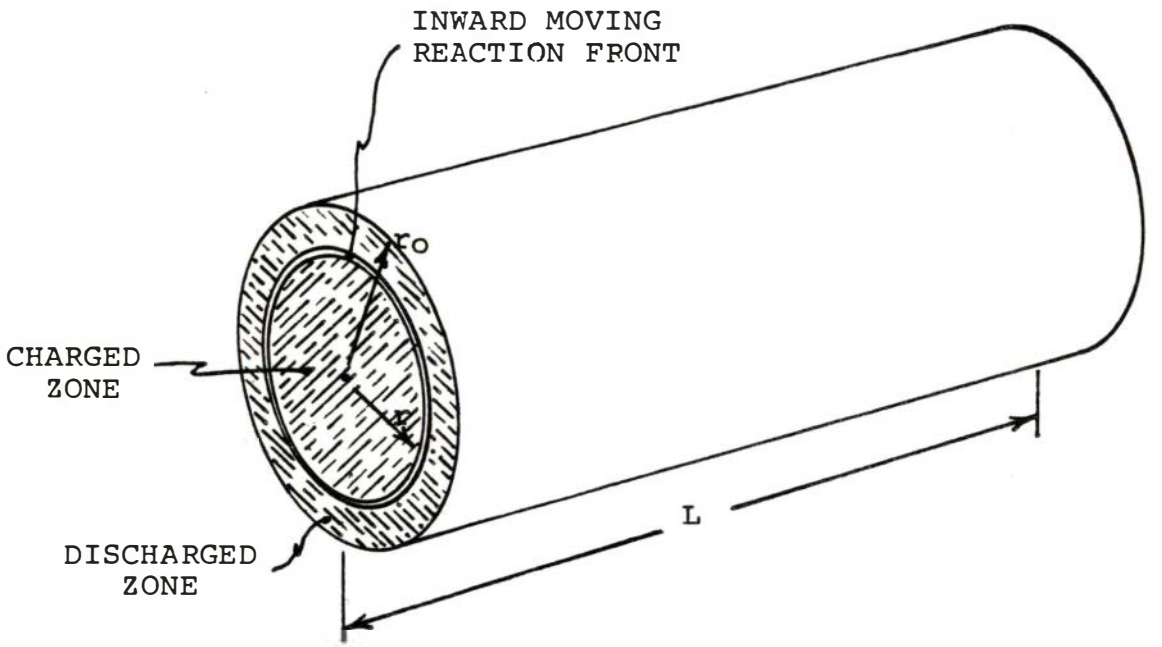

Figure 2. Schematic of the discharge process in a cylindrical metal hydride container.

This model for heat transfer and reaction was used to extrapolate the previous container's performance toward a mine-safe sub-atmospheric hydride system design. The specifications of the previous container are given below in Table 1.

Figure 3 shows the calculated effect of heat transfer enhancement on reducing the 25°C (77°F) equilibrium pressure requirements in a hydride system. A factor of 2 or 3 improvement could reduce the 25°C desorption pressure of an above-ground type hydride system to less than one atmosphere. Hydrides with less than one atmosphere of pressure at normal temperature are, of course, incapable of significant leakage in case of accidental rupture. A special module with enhanced internal heat transfer was constructed during this phase of the project. It shows a 3.7-fold improvement over previous designs.

Figure 4 shows how, if enhancement by other means is not sufficient, the tube diameter of conventional hydride systems may be reduced to achieve sub-atmospheric hydride pressures. This has the disadvantage of requiring a greater number of tubes, more joints and greater expense.

Table 1. Specifications of Previous Hydride Container Used as the Basis for the Extrapolation Study.

Type:	Tube and shell with hydride capsules (8) in tube, engine coolant in shell.		
Materials:	6061 Aluminum container 3003 H-14 Aluminum capsules 304 Stainless steel filters in capsules		
Construction:	Welded and mechanical joints		
Dimensions:	187 tubes - 135 cm x 2.86 cm x 0.124 cm wall (53.1 in. x 1.125 in. x 0.049 in. wall) Shell O.D. - 48.8 cm (19.2 in.) Overall length - 137 cm (54 in.) External tube surface area - 22.7 M^2 (244 $ft.^2$)		
Mass:			
	Hydride Alloy	318 Kg	(700 lb.)
	Container	115 Kg	(253 lb.)
	Liquid (as water)	84 Kg	(185 lb.)
	Hydrogen capacity	5.13 Kg	(11.3 lb.)
	Total	522 Kg	(1149 lb.)
	Hydrogen Mass-Percent	0.98%	
Hydride Alloy:			
	Composition	$Ti(Fe_{0.9}Mn_{0.1})$	
	Heat Treatment	None	
	Nominal Desorption Pressure at 25°C - 3.1 Atm (45.6 psia) (lower plateau used for extrapolation)		
	Heat of Reaction	7 Kcal/gm-mole H_2	
Heat Capacities:			
	Hydride Alloy, charged	70.8 Kcal/°C	
	Hydride Alloy, discharged	38.8 Kcal/°C	
	Container	23.6 Kcal/°C	
	Liquid (as water)	84 Kcal/°C	
	Cp ratio = $\frac{\text{Total Cp}}{\text{Hydride Cp}}$ =	2.52	

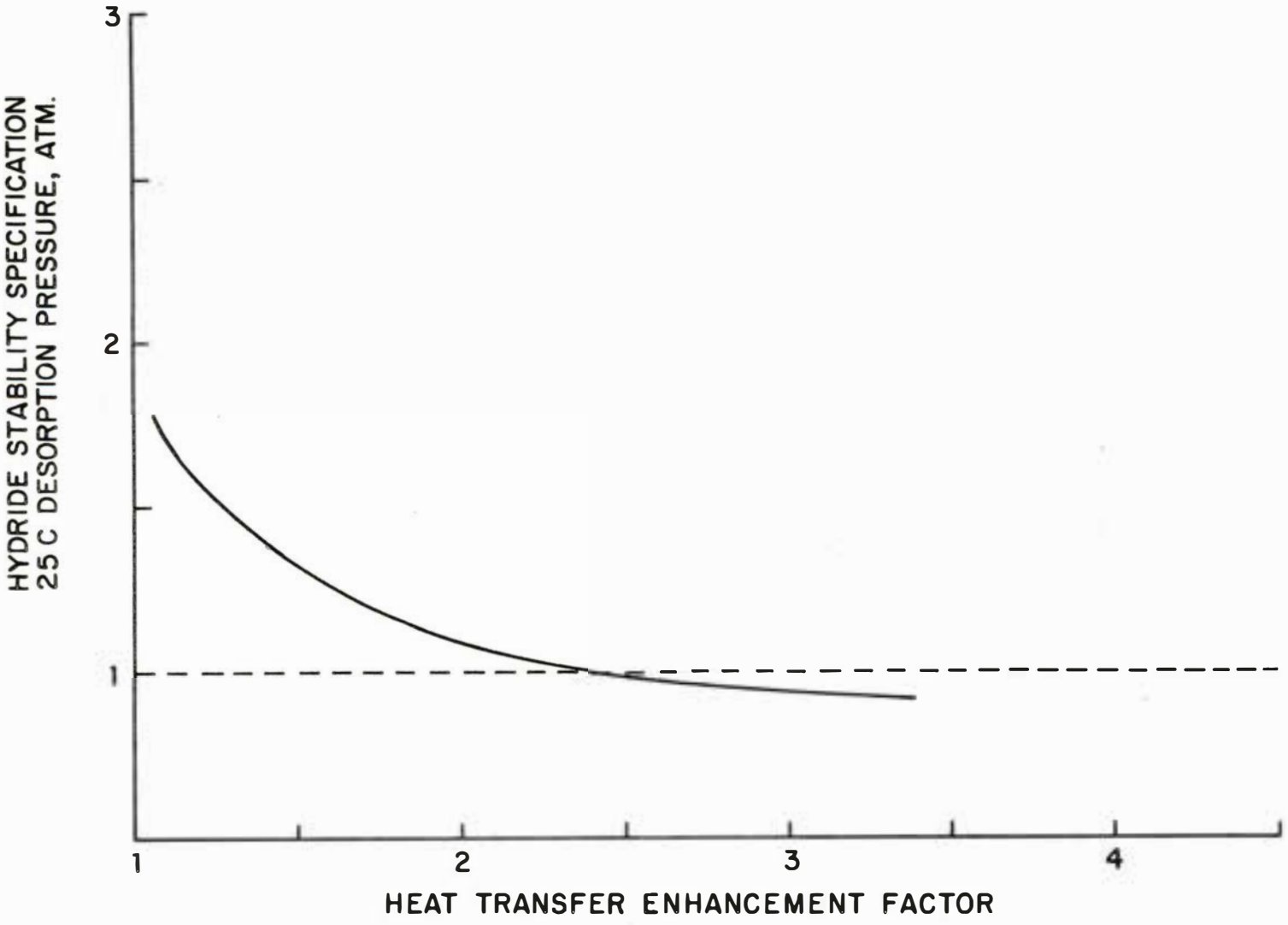

Figure 3. Plotting stability requirement vs. heat transfer enhancement shows how a safe, subatmospheric design can result from better heat transfer.

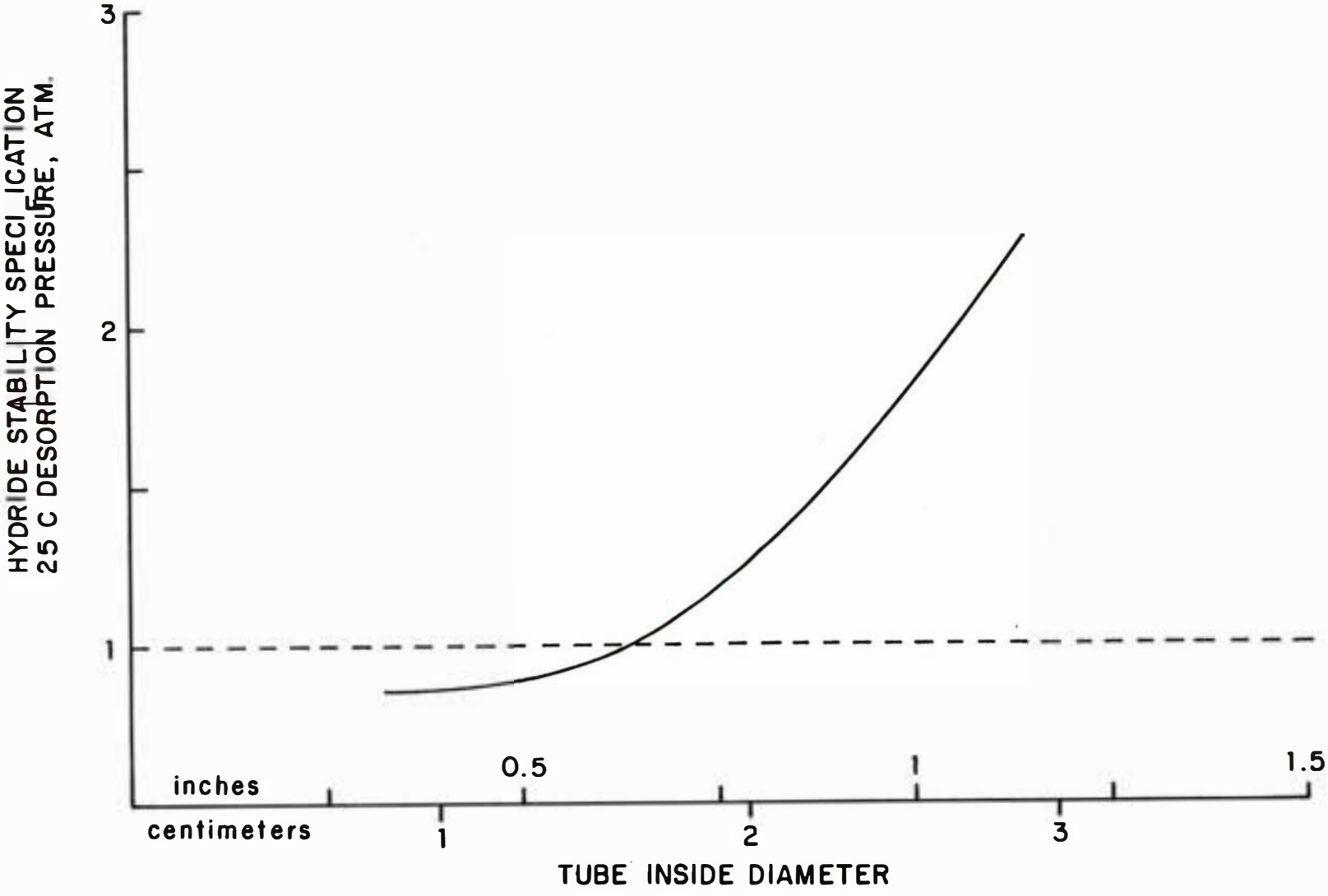

Figure 4. If heat transfer enhancement by other means is not sufficient, decreasing the diameter of the heat exchanger tubing rapidly reduces the 25°C desorption pressure requirement.

One alternative to better heat transfer is simply to increase the temperature of the heating fluid. Figure 5 shows how sub-atmospheric hydride systems may be used by raising fluid temperature to about 90°C (194°F).

The use of exhaust heat recovery devices was evaluated to some extent in hopes that higher fluid temperatures would be available without increasing engine jacket temperature. This was not fruitful. Such heat exchangers are massive, expensive and subject to thermal stress and other problems due to the high temperature of the exhaust.

The two most practical and most fruitful ways to improve the performance of the hydride containers are; increased engine coolant temperature and enhanced internal heat transfer. Both of these methods were explored during this phase of the project. The engine was fitted with a standard Caterpillar thermostat whose nominal opening temperature is 82°C (180°F). During Phase II testing, the engine had been run with a 71°C (160°F) thermostat in the interest of preventing preignition. This change had no adverse effect on the performance of the engine. The higher coolant temperature results in a 37% heat transfer improvement.

The greatest improvement in hydride performance was obtained by enhancing the internal heat transfer capabilities of the hydride container. Figure 6 shows the charging rates observed during experimental modeling of various candidate designs. The curve labeled "Standard Capsule" describes the charging of a conventional, tight-fitting capsule in a copper tube under the charging conditions listed on the figure. The curve labeled "Capsule, Large Gap" shows a slower charging due to the thermal resistance of a gap between the hydride capsule and the tube. This poor performance made it necessary to alter the capsule forming dies to get a proper fit between the capsules and the larger I.D. of the stainless steel tubing to be used in the new heat exchangers.

A test was run by using a tubular filter and pouring the hydride directly into the same copper tube used to test the hydride capsule. The data were virtually the same as the "Standard Capsule" curve proving that the capsule itself is not a significant thermal resistance.

The same copper tube, with its tubular filter, was fitted with a prototype heat transfer aid which HCI had used earlier during the development of small commercial hydride containers. The heat transfer aid is a specially constructed bottle-brush with beryllium-copper alloy bristles. The high conductivity and radial orientation of these bristles contributes significantly to the charging rate of the system as demonstrated by the curve labeled "Enchanced #1" in Figure 6. The time to achieve 90% charge was reduced from 1175 seconds to 785 seconds - a 50% improvement in heat transfer rate. A second brush with higher conductivity, chromium-copper alloy bristles was used to generate the curve labeled "Enchanced #2) in Figure 6. The resulting charging rate was 367% faster than the "Standard Capsule" curve at the 90% charged point.

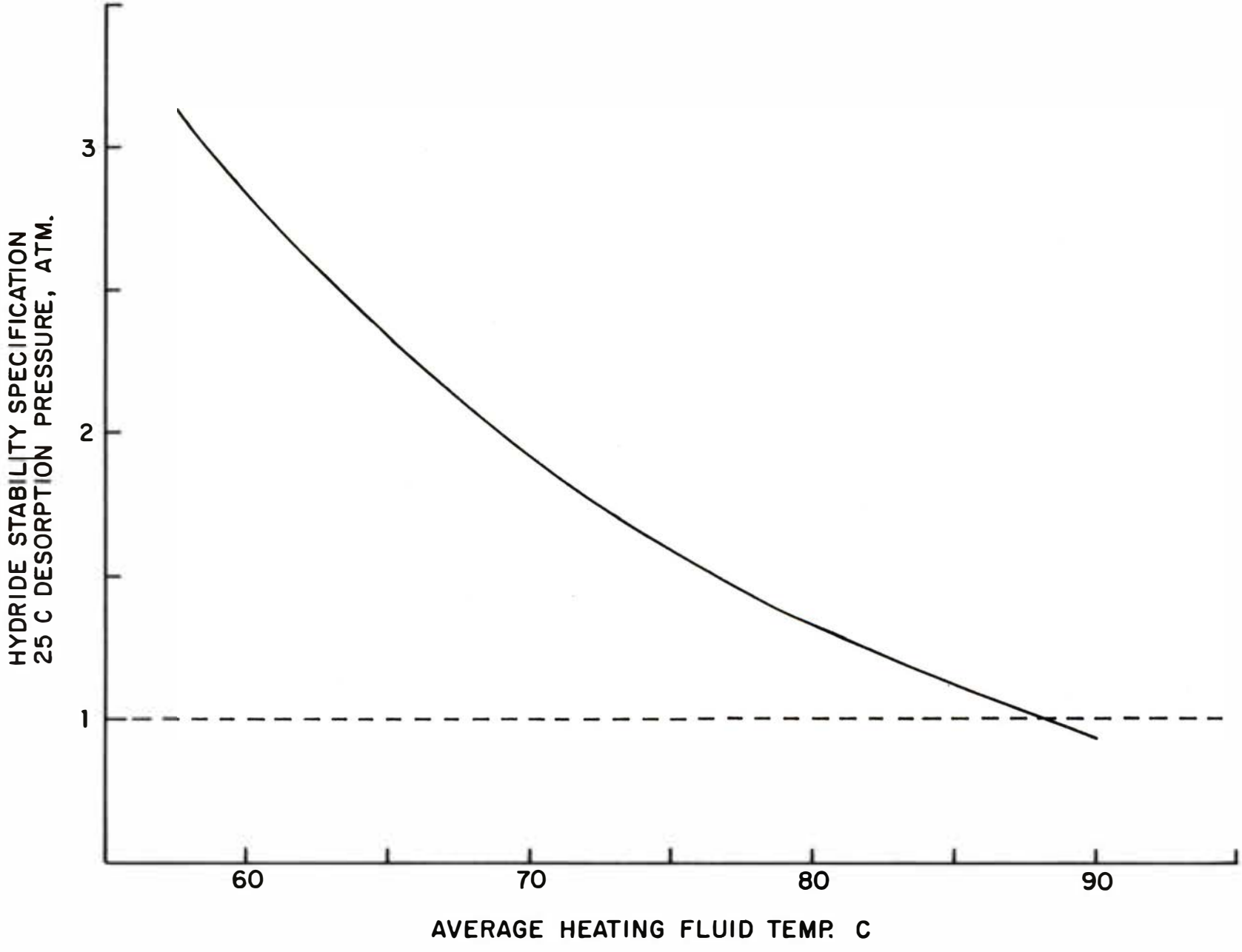

Figure 5. Raising the temperature of the heating fluid (engine coolant) has a direct influence in reducing the pressure of the hydride.

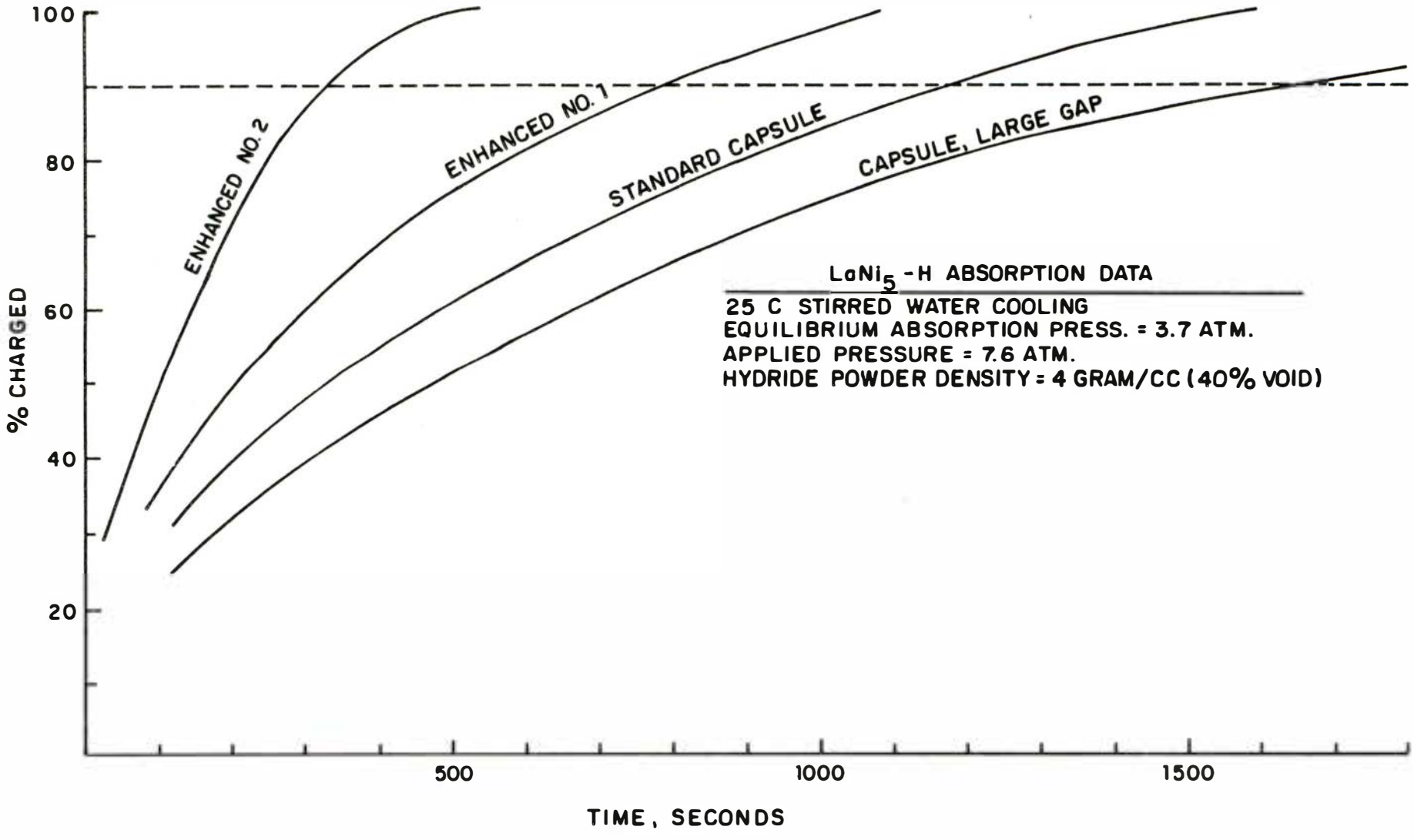

Figure 6. Charging curves under the conditions listed on the plot are a good indicator of heat transfer rate. Improvements shown are: reduced gap between capsule and tube wall, addition of a Be-Cu brush (Enhanced No. 1) and a denser, higher conductivity, Cr-Cu brush (Enhanced No. 2).

The compound improvement resulting from increased coolant temperature (37%) and heat transfer enhancement (367%) is just over 500%. This allows the engine to receive adequate fuel flow from a container about one-fifth as large as with the older design.

To determine the resulting improvement in fuel system safety, the methods of Reference 4 may be used to estimate the maximum fuel loss potential of a hydride system designed in this way. A fuel system which utilized this approach would be segmented into several modules each of which can supply the fuel demand of the engine. These modules would be heated in series fashion, one after the other. The metal hydride within the container would need to provide 3.5 atm of hydrogen pressure at its normal operating temperature (approx. 75^{o}C).

During a worst-case accident in which the fuel system is ruptured, only the active module could release fuel. The yet-to-be-heated modules do not have a positive pressure at room temperature. The hot modules, already depleted, are no longer of any safety concern.

The methods of Reference 4, also discussed in Appendix B, indicate that each hydride module, using the enhanced design discussed above, could contain up to 0.84Kg of hydrogen without exceeding the "glass-box" safety criterion. This corresponds to a hydride alloy mass of about 70Kg (depending on the alloy selected).

The full-scale tests of the enhanced design, reported in the appendix, showed a specific engine power capability of 0.80 kW per Kg of alloy. Thus, the enhanced design could serve a continuous power demand of 70 Kg x 0.80 kW/Kg = 56 KW and remain within the safety specifications.

A utility vehicle equipped with a 75 kW engine subjected to a load factor of 30% requires an average power of 22.5 kW. The enhanced modular design can safely supply the average fuel demands of a utility vehicle with a respectable margin of reserve capacity.

MODULAR HYDRIDE CONTAINER CONSTRUCTION

The container type which was used for this project is shown in Figure 7. It was an all-welded, stainless steel design which avoids the problems experienced with its predecessors. The system for the 3304 Caterpillar engine consisted of 14 separate modules like Figure 7. Each module was 2.77 M (109 in.) long and 8.9 cm (3.5 in.) in diameter. With minor modifications, these modules will fit between the framerails on the trailer of a utility truck, thus requiring no sacrifice of useful space on the vehicle. The

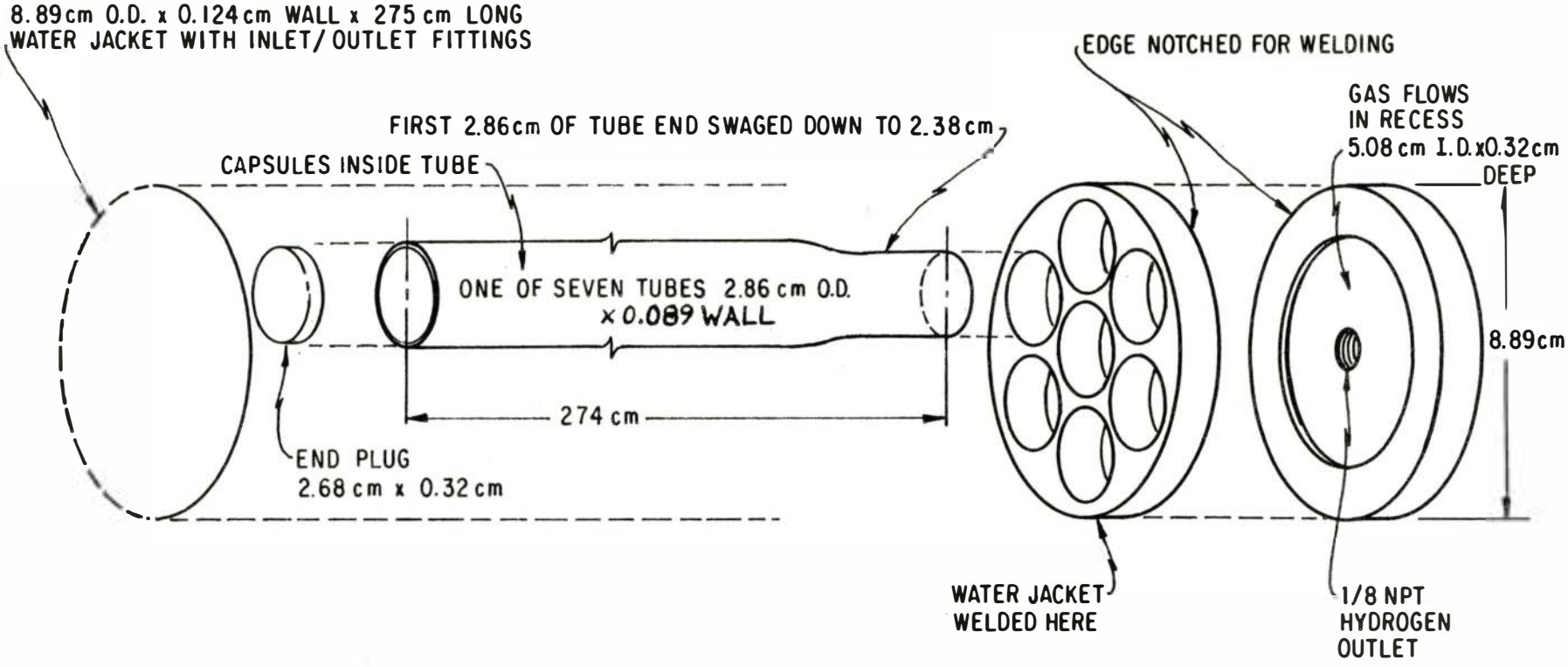

Figure 7. Schematic of heat exchanger module as constructed during this project phase.

heat exchange tubes are 2.86 cm (1.125 in.) O.D. x .089 cm (0.035 in.) wall thickness. This is thinner tubing than used in previous copper or aluminum systems but the pressure rating is similar, owing to the higher strength of 304 stainless steel. The thinner tubing necessitated new dies for the hydride capsules since inside clearances between the capsule and tube lead to poor thermal contact. Tests showed a 40% loss in heat flow when standard-size capsules were used in the larger I.D. tubing (See Figure 6).

The tubes are swaged at one end to allow them to be closely packed in the bundle. This eliminates excess water volume which previous units contained due to gaps between each tube and the next. This also leads to a more compact design.

The modules also reduce the risk of leakage experienced with earlier designs in two ways. First, they are constructed so that all joints are accessible for repair by relatively simple disassembly steps. Secondly, if a non-repairable problem develops in one of the modules, that unit may be discarded without the expense of replacing the whole hydride system.

A few model systems were constructed during the first weeks of the project to test the pressure design, weld integrity and flow characteristics. All went well except that it was found necessary to swage the tubes further back from the header end than anticipated, to get good liquid flow distribution among the seven tubes where they join the header.

The construction of the containers was done concurrently with the enhancement studies reported in the previous section of this report. This, of course, means that some of the improved heat transfer methods were not used for the 14 modules constructed during this phase of the project. It was decided, during the planning stages of the project, that it would be too time-consuming to try to develop the containers and construct them in a subsequent project phase. This would have delayed the surface demonstration for about 1 year while the development work went on to produce advanced containers. The advanced design is unnecessary for above-ground testing.

Despite this concurrent development schedule, as many of the advanced features as possible were incorporated in the hydride system, and the modular design is a step toward the mine-safe "milk-bottle" concept. The use of two different hydrides - one for cold starting, another for normal operation, is also in the interest of limiting accidental fuel release potential. The system's 14 modules are partitioned into two sets - 2 modules for cold-starting and 12 modules for normal operation. The details of the hydride modules are summarized in Table 2. The modular stainless steel containers have less hydrogen capacity per unit of weight than the earlier design. About half of the difference results from the higher capacity of the alloy used in the earlier

Table 2. Specifications of Modular Hydride System Constructed during This Project.

Type:	14 tube and shell modules with hydride capsules (8) in tube, engine coolant in shell.	
	12 modules comprise the main system.	
	2 modules are for cold start-up	
Materials:	304 stainless steel container 3003 H-14 Aluminum capsules 304 Stainless steel filters in capsules	
Construction:	All joints TIG-welded	
Dimensions:	7 tubes per module	
	274 cm x 2.86 cm O.D. x 0.089 cm wall (108 in. x 1.125 in. O.D. x 0.035 in. wall)	
	Shell O.D. - 8.89 cm (3.5 in.)	
	Overall length - 277.2 cm (109.1 in.)	
Effective External tube surface area:	1.7 M^2 (18.3 $ft.^2$) per module	
Mass per module:		
Hydride Alloy	33.9 Kg	(74.6 lb.)
Container	22.8 Kg	(50.2 lb.)
Liquid (as water)	3.7 Kg	(8.1 lb.)
Hydrogen Capacity:		
Each Main	.437 Kg	(0.96 lb.)
Each Cold-start	.404 Kg	(0.89 lb.)
Total Mass per Module	60.8 Kg	(134 lb.)

	Main	Cold start
Calculated Hydrogen Mass-Percent:	0.72%	0.66%
Useable Hydrogen Mass-Percent during tests:	0.70%	0.70%
Hydride Alloys:		
Composition	$M^*Ni_{4.5}Al_{0.5}$	$M^*Ni_{4.17}Fe_{0.83}$
Heat Treatment	Solution Anneal	None
25°C Nom. Desorp. Pressure	3.4 Atm(48.5 psia)	10.3 Atm(154 psia)
Hysteresis Pressure Ratio	1.12	1.18
Heat of Reaction per g-mole H_2	6.7 Kcal	6.3 Kcal
Heat Capacities:		
Hydride Alloy, charged	5.63 Kcal/°C	5.49 Kcal/°C
Hydride Alloy, discharged	3.05 Kcal/°C	2.98 Kcal/°C
Container	2.74 Kcal/°C	
Liquid (as water)	3.7 Kcal/°C	
Cp ratio = $\frac{\text{Total Cp}}{\text{Hydride Cp}}$ =	2.14	

* M denotes mischmetal, a group of rare-earth elements which occur naturally in ore.

design ($Fe_{0.9}Mn_{0.1}Ti$) compared to the mischmetal-nickel based alloys in the modular system. The balance of the decrease in weight-percent hydrogen results from the greater density of stainless steel compared to the aluminum used previously. Hydride isotherms for the two alloys are shown in Figures 8 and 9.

The 14 hydride modules are enclosed in plastic foam type building insulation 2.5 cm (1 inch) thick. This material has an insulation rating of R-8. The need for insulation was apparent from earlier tests conducted on a highway vehicle with a hydride fuel system. Without insulation, a sizeable fraction of the engine's heat was lost from the surfaces of the hydride system. This reduces the heating rate of the hydride system to an unacceptable extent, especially at low ambient temperatures.

HYDROGEN AND COOLANT CONTROLS

Figure 10 is a schematic of the hydrogen and coolant plumbing and controls which coordinate the operation of the hydride system with the fuel and cooling demands of the engine.

The hydride system is divided into two parts: the main system and the cold-start system. Each of these has its own coolant controls and hydrogen controls. The hydrogen system will be described first.

The main pressure regulator, PR1 was set at a higher output pressure, (typically 60 psig) than the cold-start regulator, PR2 (typically 50 psig). Therefore, whenever hydrogen was available from the main hydride system the cold start system was not discharged.

If the temperature was too low for the main hydride system to supply the engine with fuel, the pressure fell to a lower value at which time the cold-start regulator, PR2, began to flow hydrogen. The cold-start hydride system has a less stable hydride in it, so it is capable of supplying useful hydrogen pressure at a much lower temperature than the main hydride.

After the engine coolant reached 71^{o}C (160^{o}F), the thermostat opened and the main hydride began heating until it produced a pressure greater than the setting of the cold-start regulator. Fuel then stopped flowing from the cold-start system and began flowing from the main system. However, if the main system failed to provide sufficient pressure for any reason (running low on fuel, for example), the cold-start regulator began flowing again. Other features of the hydrogen system are: refueling quick-connects, QC1 and QC2; 3.5 MPa over-pressure reliefs, R1 & R2; filters, F1 & F2 and manual shut-off valves, V1 & V2. Manual valve, V6, was added midway through the test series to facilitate certain procedures such as parallel refueling tests. V6 directly connects the main and cold-start hydrogen systems upstream from their regulators.

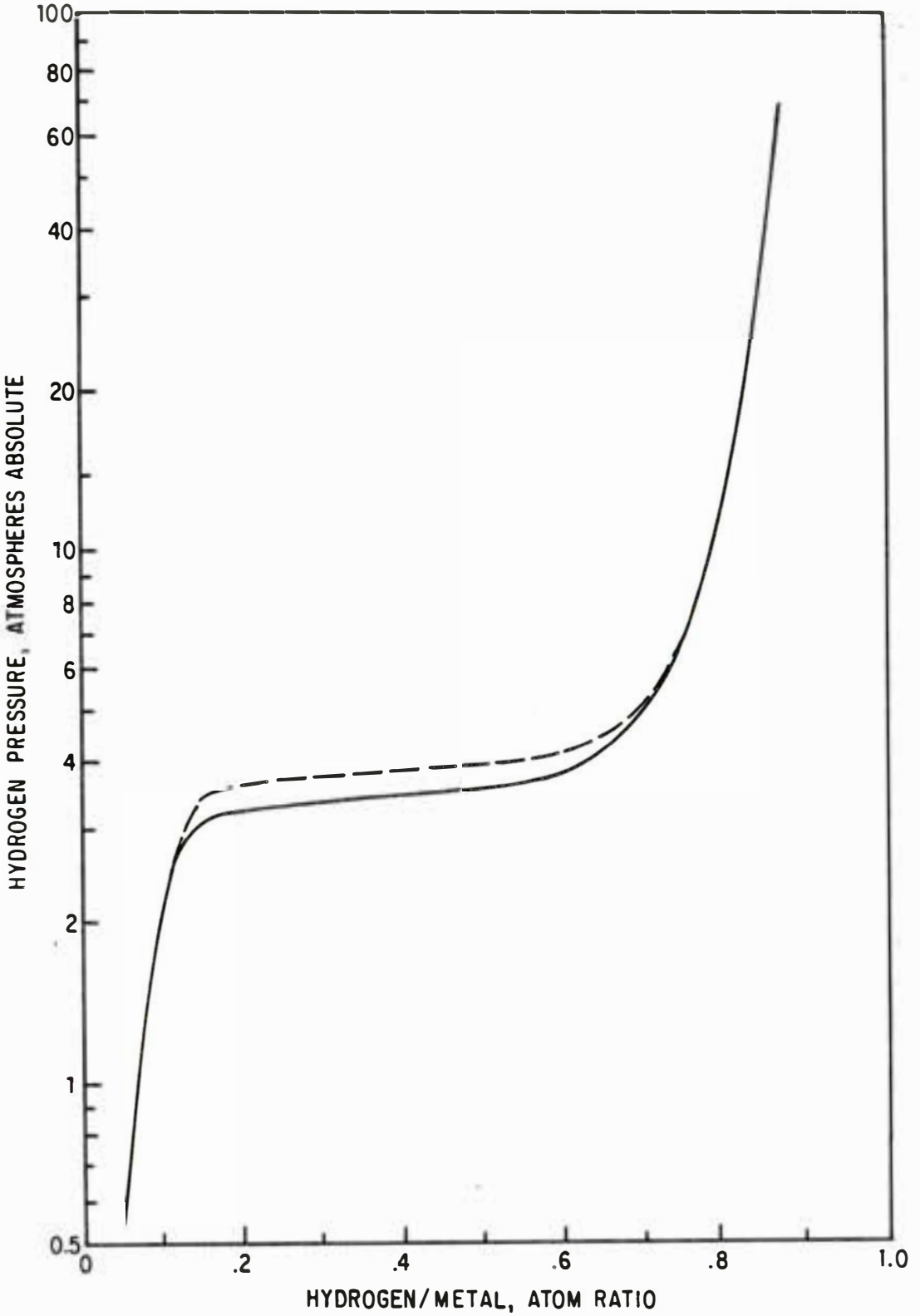

Figure 8. 25°C desorption (solid curve) and absorption (dashed curve) isotherms for the hydride used in the main system, $MNi_{4.5}Al_{0.5}$-H.

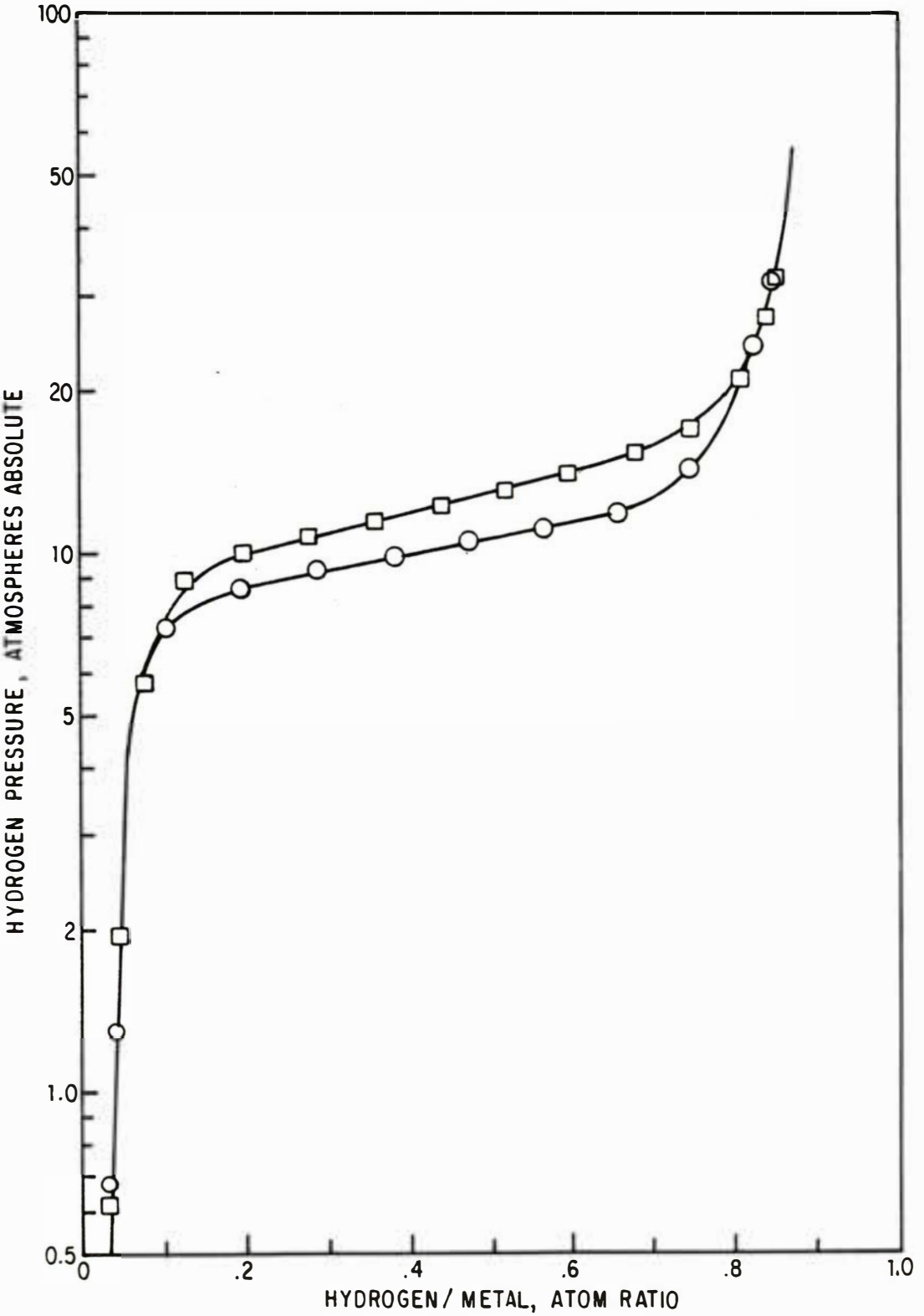

Figure 9. 25°C desorption (circles) and absorption (squares) for the hydride used in the cold-start system, $MNi_{4.17}Fe_{0.83}$-H.

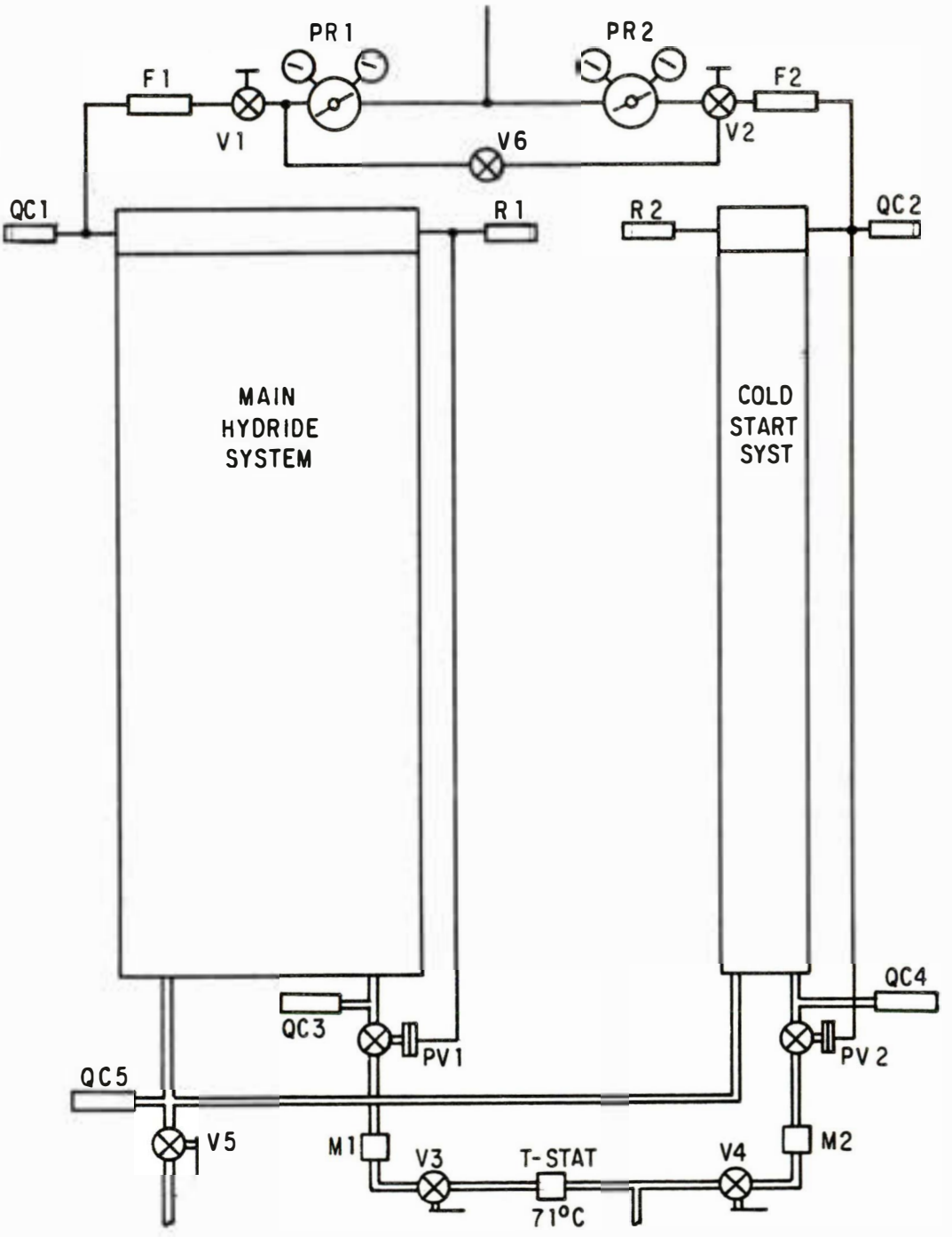

Figure 10. Schematic of the liquid and hydrogen plumbing systems assembled during this project. Components are described in the text.

The coolant control system had the following priorities built into it. The first priority for heat from the engine's coolant was the cold-start hydride. Regardless of engine temperature, the coolant passed at maximum flow through the cold-start hydride system whenever its pressure was less than the setting of the pressure-operated coolant control valve, PV2.

The next priority for heat was the engine itself. Extended running at low jacket temperatures will cause condensation in the crankcase which can lead to lubricant degradation and metal corrosion.

After the engine warmed up, the 71°C (160°F) thermostat opened, permitting some of the coolant to enter the main hydride system. Eventually the fuel demand on the cold-start hydride ceased, as previously explained. Pressure then increased inside the cold-start system until the pressure-operated coolant control valve, PV2 closed. PV2 prevented excessive pressure from building up in the cold-start hydride.

The energy demand of the hydride system is less than the energy available from the engine coolant. Therefore the temperature continued to rise in the main hydride system. This temperature rise was limited by two additional features of the coolant control system. The main hydride had a pressure-operated coolant control valve, PV1 which works just like the corresponding valve, PV2 on the cold-start hydride. If, for any reason, the pressure increased beyond the desired value, PV1 closed preventing additional hot fluid from entering the main heat exchanger. PV1 and PV2 were set at about 1.1MPa gage (160 psig) to give adequate operating pressure for regulators PR1 and PR2 and yet maintain a safe margin below the 3.5 MPa relief valves, R1 and R2.

When the system was fully warmed-up, the pressure control valves, PV1 and PV2 limited the flow of coolant into the hydride system. The engine then continued to heat until it opened the engine thermostat at 82°C (180°F) and began rejecting heat to the engine cooler.

Each of the two fluid circuits also contained a calibrated orifice flowmeter, M1 and M2 in Figure 10, for monitoring the flow of coolant through the system. The pressure drops through the orifices were read from manometers at the dynamometer control panel. Flow and temperature drop were used to deduce the heat input to the hydrides.

Additional features of the coolant control system were manual shut-off valves, V3, V4 and V5 and quick-connects QC3, QC4 and QC5. The quick-connects were used to flow cold water in and out of the system during refueling. Not shown in Figure 1 are several thermocouples placed to aid in the study of the running and refueling processes.

ENGINE TEST RESULTS

A series of 14 tests were conducted by equilibrating the engine and hydride system at the "cold-start" temperature, (5-20°C) starting the engine with fuel from the hydride system, idling for 30 seconds and then establishing the test speed and load. The operating conditions were the following:

Table 3. Engine Test Conditions During 14 Test Runs With The New Metal Hydride System.

Test No.	Speed, RPM	BMEP, kPa	Power, kW	Cold Start Temp. °C
1.	600	5	0.2	5
2.	1400	6	0.5	5
3.	1400	149	12.1	5
4.	1400	406	33.0	15
5.	1400	704	57.2	6
6.	1800	4	0.5	20
7.	1800	164	17.2	19
8.	1800	542	56.7	20
9.	1800	699	73.0	5
10.	1800	704	73.6	20
11.	2200	4	0.7	20
12.	2200	242	30.9	20
13.	2200	373	47.6	20
14.	2200	622	79.4	20

In each case the hydride was saturated at the beginning of the test at the temperature shown in Table 3 and at a pressure between 2070 and 2760 kPa gage (300-400 psig). The lower starting pressures correspond to 5-6°C cold-start tests. Later, when it became necessary to start at 20°C for the higher powered tests, the hydrogen pressure inside the hydride container rose as the saturated hydride was warmed prior to the start of the test. In all cases, however, the hydrogen content of the system was nearly the same at the start of each test.

When the engine would no longer hold the speed and load toward the end of each test, the load was removed and the engine was idled at 600 RPM for 30 seconds. The idling condition consumes so little fuel that 30 seconds of idling before and after each

test has an insignificant effect on total fuel consumption. The engine could idle at 600 RPM for 16 hours and 31 minutes before depleting the hydride. Therefore, the two 30-second idling periods represent about 0.1% of the total fuel consumed during a test.

Figure 11 shows the variations in temperature, waterflow, heat input and hydrogen pressure during a typical test (No. 8). It may be helpful to refer back to the plumbing schematic, Figure 10, to understand the shapes of these curves.

The temperature of the engine coolant rises rapidly at the start of the test since only a trickle (100 cc/sec) is going to the hydride system during the first 8 minutes of the run. This small bypass flow is permitted so that the 71°C (160°F) hydride thermostat is heated to the engine temperature without much delay. The hydrogen pressure falls during this initial period since very little heating is applied by the engine. The intent of heating the engine as quickly as possible is to avoid condensation in the crankcase.

For the first 6 minutes of engine test #8, the cold-start system is completely inactive. The main system supplies gas to the engine as its pressure and temperature fall. At 6 minutes, the main hydride is no longer capable of flowing hydrogen at the required rate. This is when the cold-start system is needed. The pressure in the fuel line falls below the setting of the cold start regulator (PR2 in Figure 10) and gas begins to flow from the cold-start modules to supplement the dwindling flow from the main hydride system. At 8 minutes, the pressure operated coolant valve (PV2 in Figure 10) senses the pressure drop in the cold-start system and opens, allowing fluid from the engine to enter the cold-start hydride modules. The surge of cold fluid returning to the engine from the cold-start modules is seen as a sudden decrease in engine temperature at 9 minutes. The corresponding "bumps" in the flow and energy curves of Figure 11 are also noteworthy.

By the 11th minute, the cold-start system is no longer needed. PV2 in Figure 10 is nearly closed and the main hydride is once again providing most of the fuel. The main bed steadily gains temperature and pressure as it absorbs all of the waste heat available from the engine until the 22nd minute. The main flow is increasing during this period as the 71°C (160°F) thermostat progressively opens.

At 22 minutes the engine's 82°C (180°F) thermostat begins to open, rejecting heat to the engine cooler.

From 22 minutes to 28 minutes, the main hydride continues to heat with a corresponding rise in pressure until the pressure-operated coolant valve (PV1 in Figure 10) is on the verge of closing. If the pressure had risen much past 1100 kPa gage (160 psig), the coolant flow to the main hydride would have been cut off by PV1 (See Figure 10).

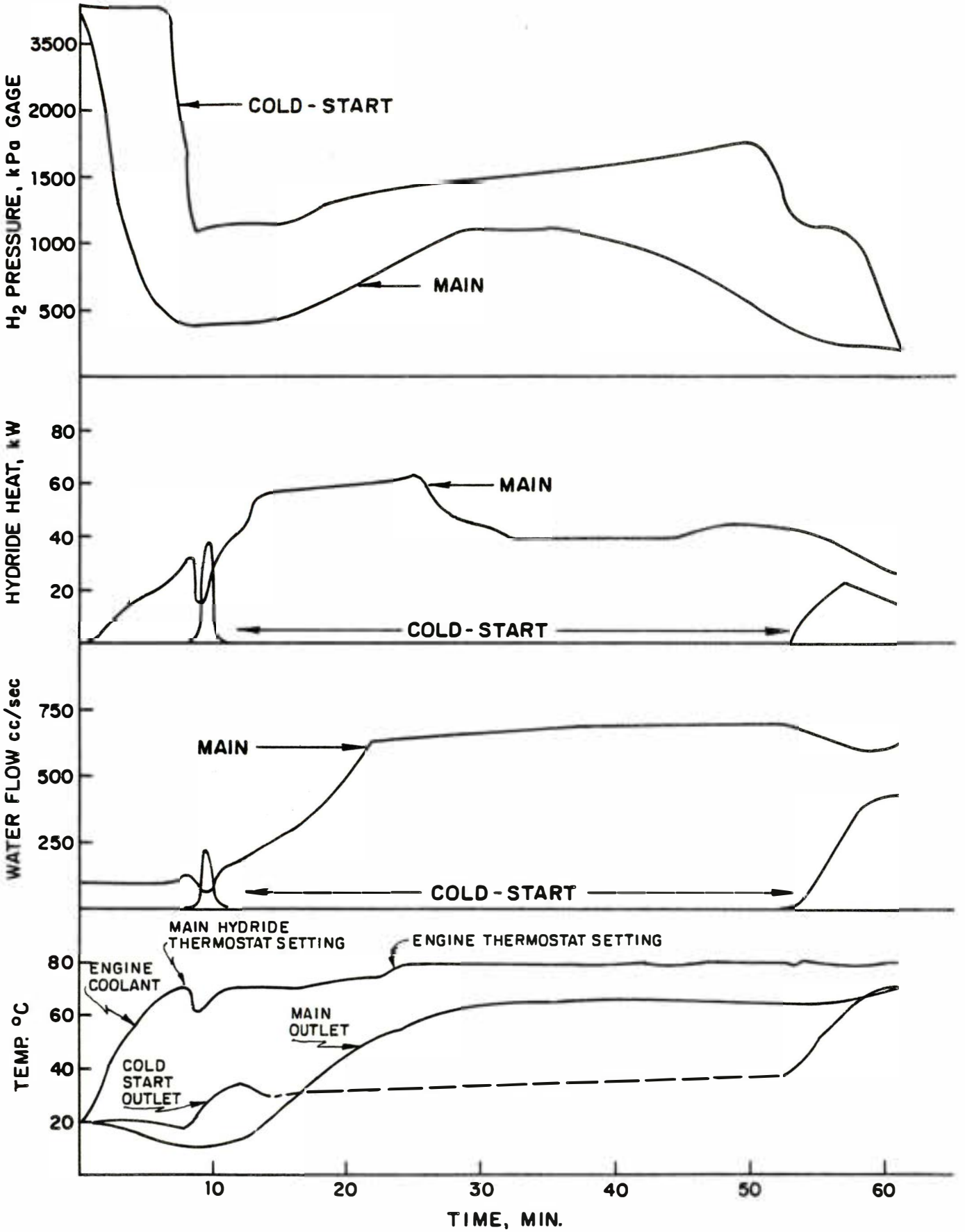

Figure 11. Variations in temperature, water flow heat input to the hydride and hydrogen pressure during a typical test run (56.7 kW, 1800 RPM).

During this period, the cold-start system is inactive except for a slow rise in temperature and pressure. This is due to conducted heat from the main hydride. When this system is installed on the utility truck, the cold-start system should be separated from the main hydride by insulation. During some of the longer tests it became necessary to manually bleed pressure from the cold-start hydride into the main hydride through V6 to prevent excessive pressure build-up.

From about 32 to 45 minutes everything is fairly constant except for a slow decrease in main system hydrogen pressure. This pressure drop is indicative of the thickening annular layer of depleted hydride shown schematically in Figure 2. This layer acts as a heat transfer barrier around the active material at the center of the tubes in the hydride system. As a result, the temperature (hence pressure) of the active material must decrease to sustain the required heat flow.

The heat flow during this time was about 40kW. This is nearly twice the power being consumed by the hydride reaction so it appears that heat loss from this system is still excessive despite the R-8 insulation. The insulation was left open at one end for access to the plumbing, so convective losses may have been high. Occassional water spillage in the test cell may also have contributed to the heat loss by wetting the insulation and by evaporative cooling during the run.

The refueling data, reported in a subsequent section of this report, establishes the amount of fuel used during each test. The data are plotted as shaded points in Figure 12. The other data in this figure were established by engine instrumentation. The good agreement between these two completely independent methods of determining fuel consumption is reassuring.

The running time provided by the hydride at each speed and load is plotted in Figure 13. This data will be useful for estimating the fuel system size required for a given duty-cycle and refueling interval.

Figure 14 is another way to view the data generated during this project phase. It shows clearly that the liquid flow through the hydride's heat exchanger was adequate, even at the lowest engine speeds. If external heat transfer were a limiting aspect of this hydride container design, the nearly 2:1 increase in liquid flow between the 1400 RPM and 2200 RPM data would have produced different run periods at the same fuel demand rate.

A limitation of the present design is apparent in Figure 15. At the higher fuel flows, the total fuel available from the main hydride system tapers off. If internal heat transfer were adequate, the hydrides would behave no differently from a tank of liquid fuel: the same total amount would be available regardless of flow.

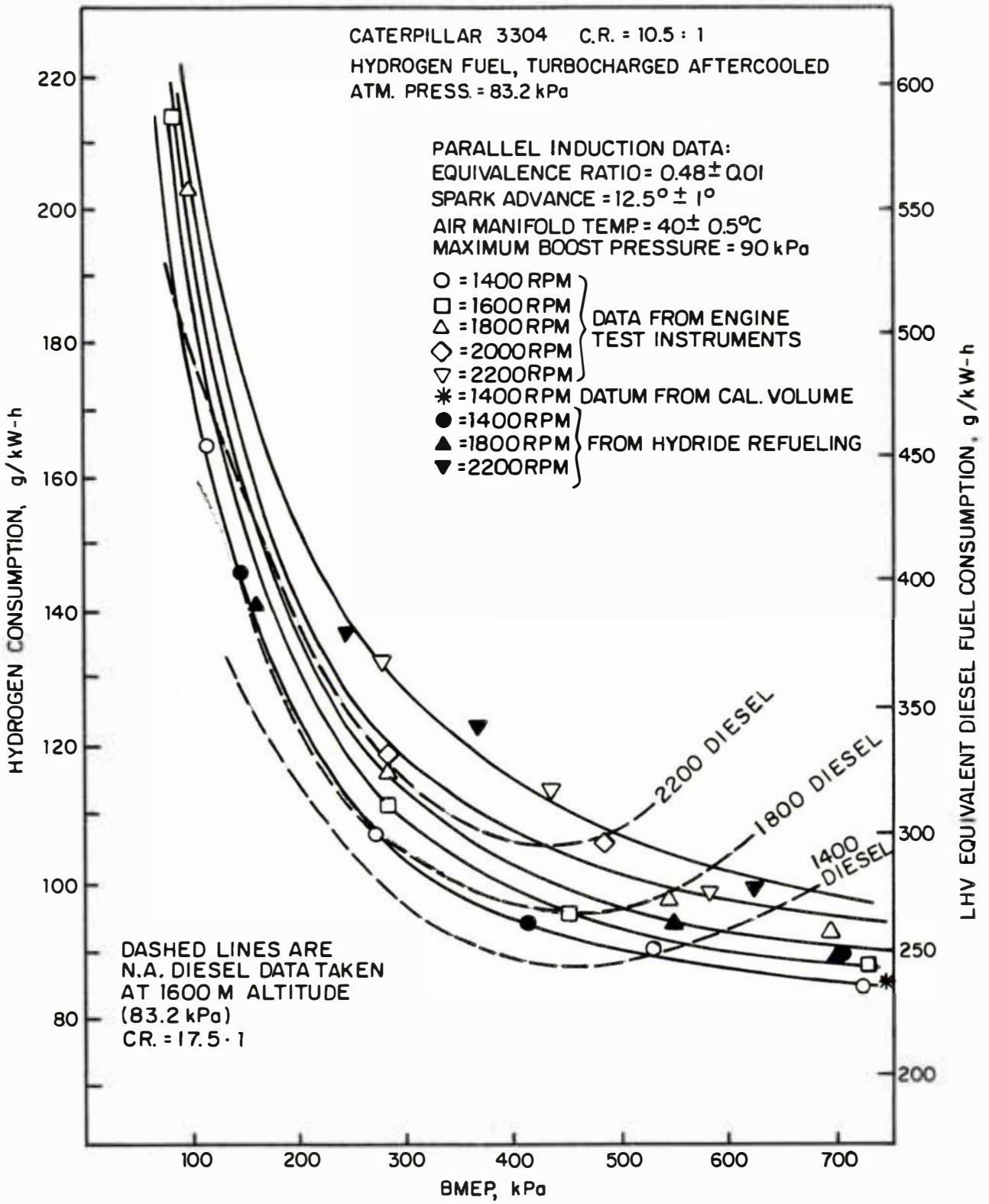

Figure 12. Brake-specific fuel consumption, determined from refueling data are in good agreement with data from engine instrumentation taken during earlier testing.

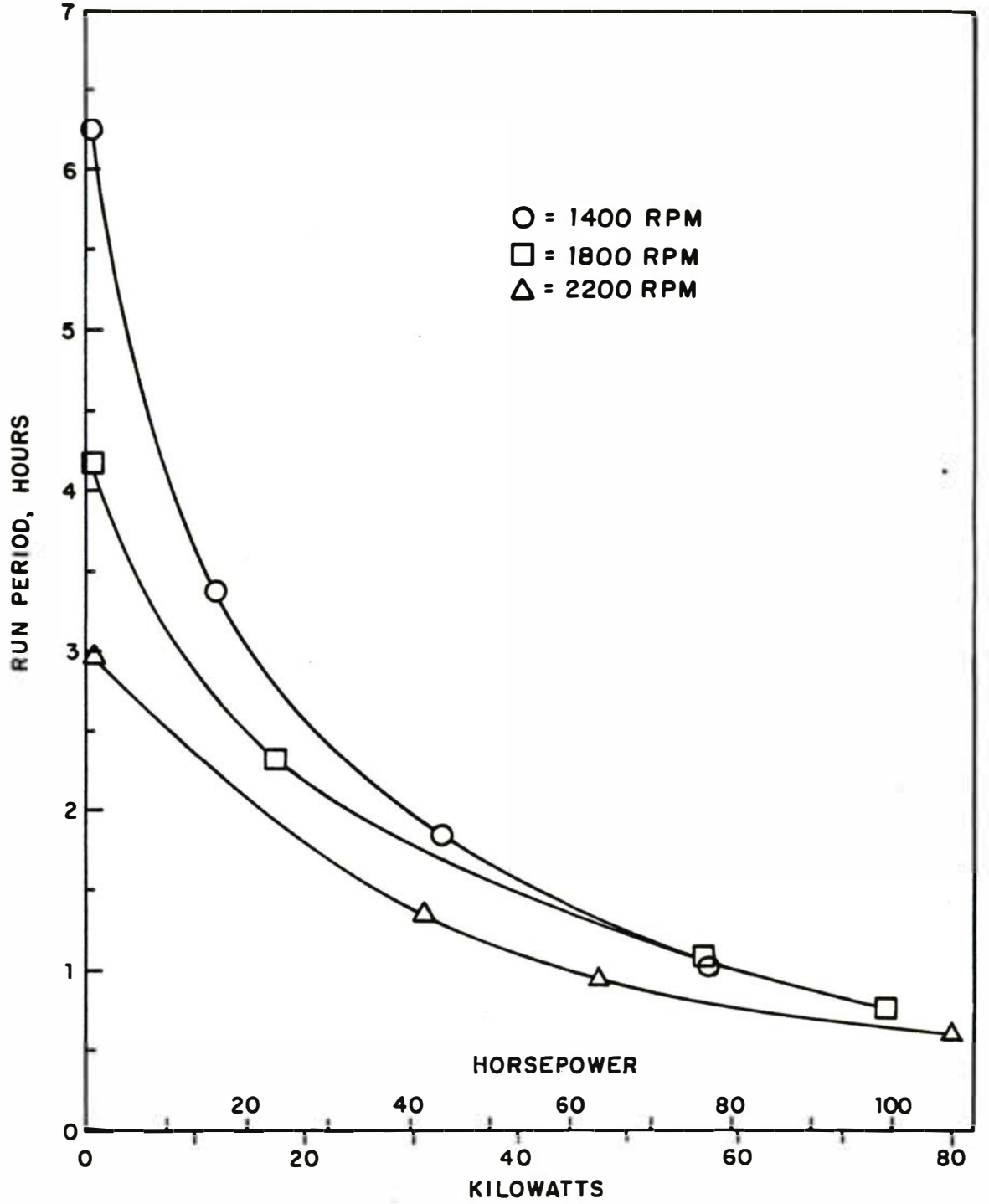

Figure 13. The run period provided by the hydride system varied according to engine power and speed.

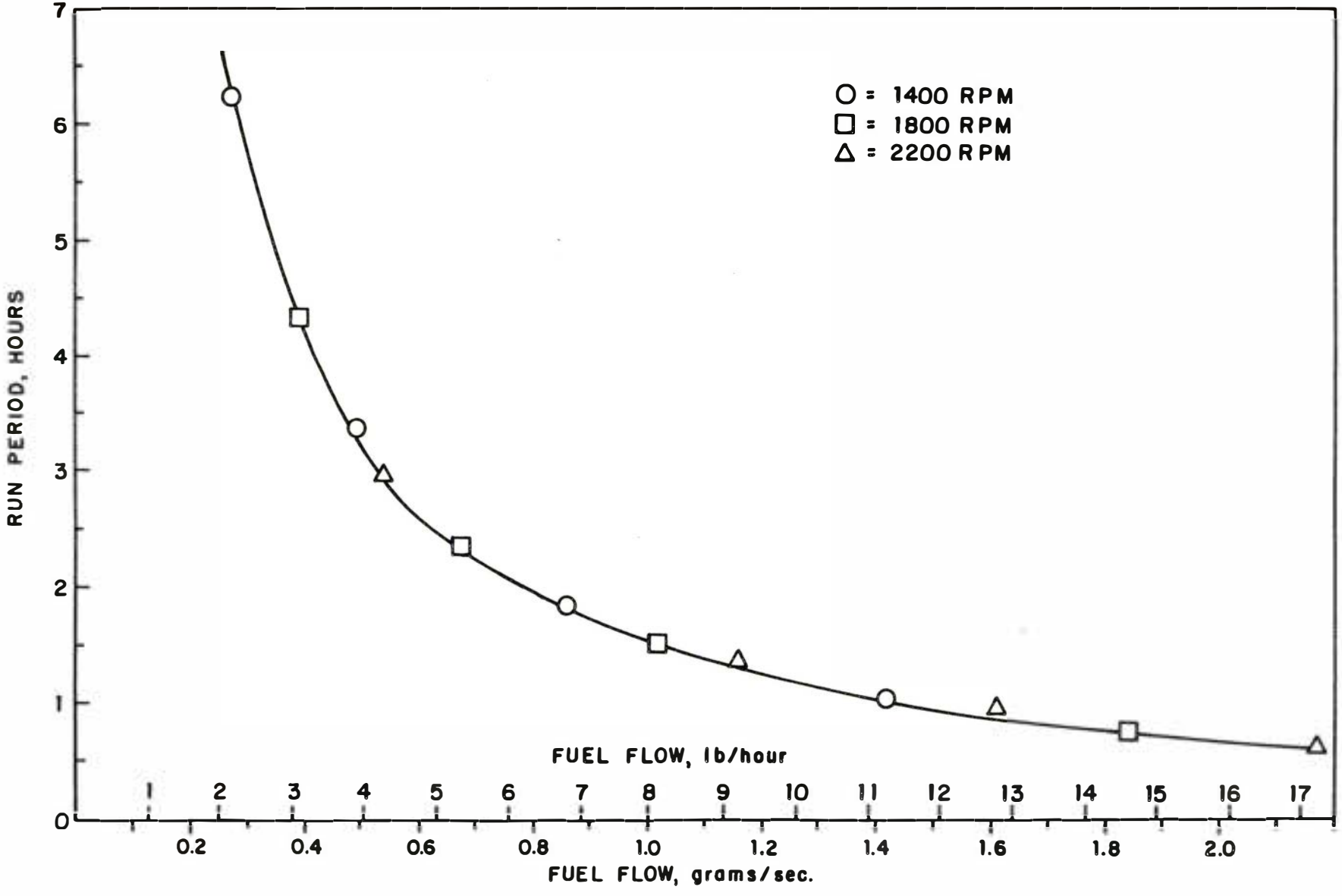

Figure 14. Run Period was directly related to fuel flow regardless of engine speed.

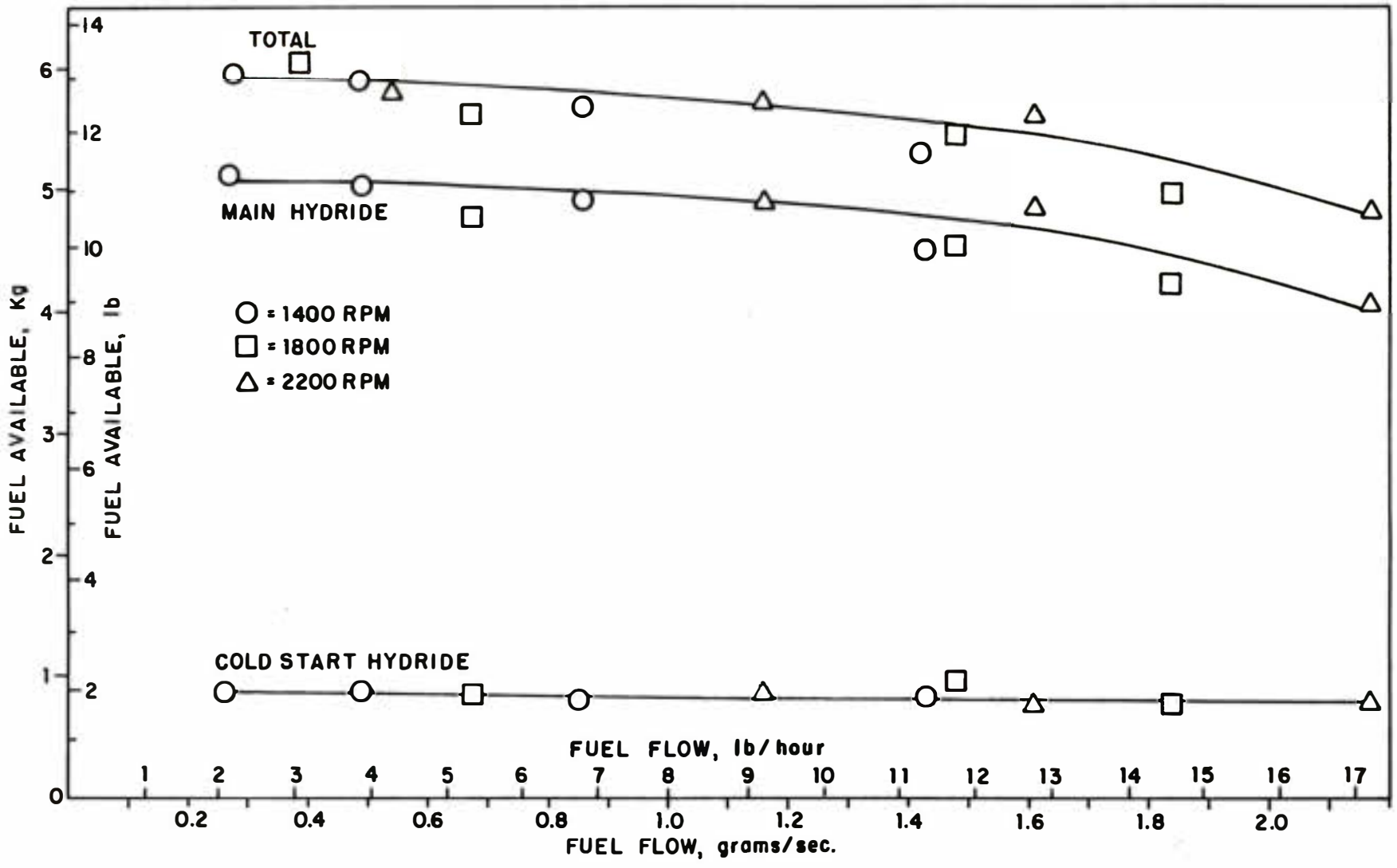

Figure 15. The total amount of fuel available from the main hydride is reduced at the higher flow conditions. This shows the limitations of heat transfer in the capsule-type hydride containers.

The cold-start system has just this property. The relatively unstable hydride can produce useful fuel pressure even when the unreacted core material (See Figure 2) drops below $0^{o}C$. With $80^{o}C$ fluid available from the engine, the ΔT is large so the cold-start system is able to deliver virtually all of its fuel even at the highest demand rates. Unfortunately, underground safety considerations limit the use of the unstable hydride materials in the cold-start system. The alternative is to improve heat transfer in other ways as discussed previously in the container design section of this report and in the Appendix.

One positive side-effect of the inability of the main hydride to deliver all of its fuel at the highest demand rates is that the vehicle operator will notice a loss in power when 10-15% of the fuel remains for returning to the fuel station.

COLD-START TESTS

One of the design objectives during this phase of development was to produce a hydride system capable of supplying the engine with fuel at low start-up temperatures. Some mines may store their vehicles during off-shift or maintenance periods in cool, outdoor locations. A target cold-start temperature of $4^{o}C$ ($40^{o}F$) was set during the planning stage of this program phase as a condition which would serve the majority of mine operations.

The cold-start alloy selected for this purpose was $M^{*}Ni_{4.17}Fe_{0.83}$ which can produce positive hydrogen pressures at temperatures below $-20^{o}C$ ($-4^{o}F$). There was never any doubt that the system would be capable of starting the engine at $4^{o}C$ ($40^{o}F$) so it was decided to learn just how much hydrogen flow could be sustained after starting at a low temperature.

The 14 tests, listed previously in Table 3, include 5 tests (1, 2, 3, 5 and 9) which began at $5-6^{o}C$ ($41-43^{o}F$) cold-start temperature. The cold-starting condition was established by flushing cold tap-water through the engine jacket and hydride heat exchangers until temperature equilibrium was attained. Among this group of tests, only test #9 failed to hold the power indicated in the table for the entire test period. Figure 11 showed temperature, flow, energy and pressure variations for a normal run during which the hydride system always provided enough fuel to the engine until nearly all of the fuel had been consumed. In test #9, the main hydride system pressure fell below the setting of the cold-start regulator (PR2 in Figure 10) and remained there until the cold-start modules were depleted of fuel. At that time (12 minutes into the test), the power began to drop due to inadequate fuel pressure.

The group of cold-start tests performed during this project phase show that the power which may be sustained continuously from a low-temperature starting condition lies between 57.2 kW (test #5)

and 73.0 kW (test #9). The engine will not only start when cold, but may be run continuously at about 3/4 load. The load-factors for various mining machinery have been estimated as follows (Ref. 4).

Personnel Carrier	10%
Utility Vehicle	30%
LHD	50%

Thus, the hydride system would serve any of these fuel demands even if started from low temperature.

FUEL SYSTEM RECHARGE TESTS

Subsequent to each engine dynamometer test, the metal hydride fuel system was recharged with hydrogen to determine the mass of fuel consumed under that particular engine speed/load/temperature condition. Additional information on the fuel system's performance was obtained during these refueling tests by varying the applied hydrogen pressure and coolant flow for both the cold-start and the main beds. In all cases, however, the metal hydride was fully recharged (saturated) so that all engine dynamometer tests were started with full fuel systems. The refueling of the cold-start system was accomplished by connecting hydrogen to QC2 as shown in Figure 10, and admitting cold tap water to QC4. The hot water leaving the system was drained through a hose connected to QC5. The main bed was refueled by applying hydrogen to QC1, and cold tap water to QC3. The drain for the main system (and cold start system) was QC5.

The hydrogen for each refueling test was provided by a 1203 m^3 tube trailer. Noting temperature from a thermocouple attached to the tube wall and recording the changes in pressure as a function of time, each refueling test also generated data on instantaneous fuel flow. Whenever possible, the high-pressure hydrogen tubes were selected so as to give the maximum pressure difference during the refueling, thereby minimizing the effect of pressure gauge inaccuracies on hydrogen mass calculations.

The flow of the tap-water coolant was nominally set for either 200, 300, 500 or 700 cc/sec by a fixed orifice in the water supply. The actual flow of water during a test was determined by noting the volume delivered through a totalizing water meter immediately upstream of the fixed orifice. The water supply delivered a nearly constant (5-6^{o}C) source for all tests. Thermocouples measured the temperature rise of the coolant through the metal hydride fuel system, thereby providing an energy balance around the recharging system.

The high pressure hydrogen was connected, through a regulator, to the fuel system by a flexible line. The regulator was manually

varied throughout the tests to maintain as constant an applied hydrogen pressure as was possible. A separate pressure gauge on the hydride system was noted during refueling tests to record the actual pressure within the hydrogen manifold.

Recharge periods for the main fuel beds (approximately 5 kg hydrogen) ranged from 700 to 1800 seconds (12 to 30 minutes), while for the cold-start system (approximately 0.8 kg hydrogen) 90% recharge periods varied from 700 to 1250 seconds (12 to 21 minutes). With both fuel systems connected, and simultaneously recharged, the refueling required 900 seconds at 2.75 MPa (400 psig).

COLD-START REFUELING

The cold-start fuel system was tested under 12 various conditions of hydrogen pressure (2.07, 2.40, 2.75 MPa) and coolant flow (200, 300, 500 and 700 cc/sec). The data and results from a typical refueling test are shown in Figure 16, in which 528 cc/sec of coolant and 2.75 MPa (400 psig) of hydrogen pressure set the condition. Proceeding first to the bottom curve in Figure 16, it can be noted that the applied hydrogen pressure quickly raises the pressure in the system. This was always found in the cold-start refueling tests, but as will be shown later, the quick rise in hydrogen pressure was rarely found during the main bed tests.

The curves which show the coolant temperatures during the refueling are immediately above the pressure curve. The inlet water temperature was a constant 6^{o}C, while the outlet peaks at over 20^{o}C and slowly approaches the inlet temperature. The equilibrium absorption temperature for the cold-start hydride corresponding to an applied pressure of 2.75 MPa is 46^{o}C. The equilibrium temperature for 2.07 MPa is 37.7^{o}C, while at 2.40 MPa it is 42.6^{o}C.

The percent-charged curve shows that this refueling required 711 seconds to recharge to 90% of capacity. This is one of the quicker recharge runs, compared to other recharge periods of up to 1255 seconds. All refueling runs exhibit the slow approach to 100% saturation. By convention, metal hydride recharge data are always presented on a time-to-90% basis since it is considered more representative of the majority of the refueling process.

The uppermost curves in Figure 16 are perhaps the most interesting. The curve labeled "Heat Rejected to Coolant" is obtained from the inlet and outlet coolant temperatures and the coolant flow. However, calculation of the "Heat of Reaction" is not as straightforward. The data points on this curve actually represent the average heat produced by the absorption reaction during a measured period. These values were obtained by multiplying the heat of reaction (6.2 kcal/mole of hydrogen) by the number of moles of hydrogen withdrawn from the tube trailer during a 60, 120 or 240 second period.

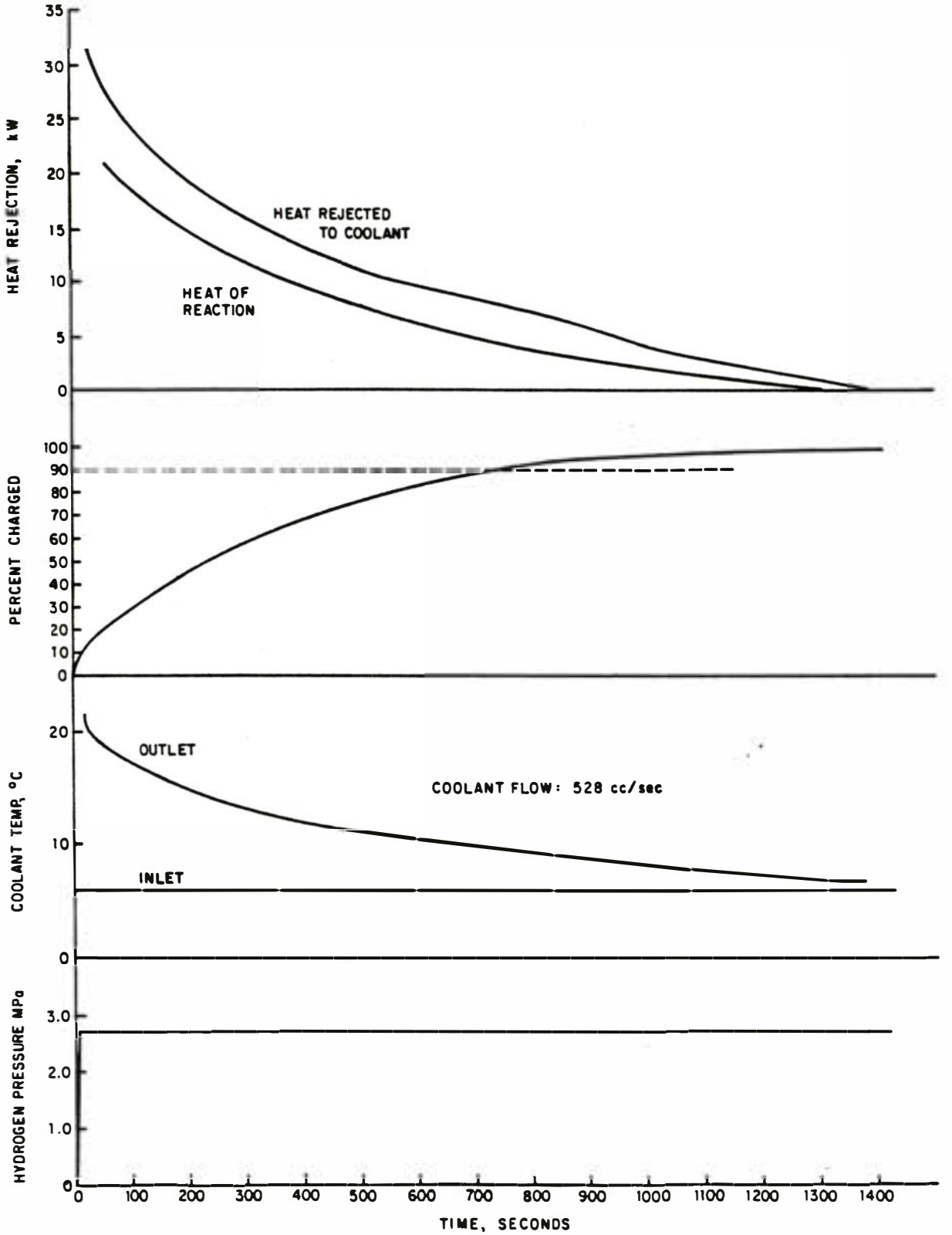

Figure 16. Hydrogen pressure, coolant temperature, fraction charged and heat flows during recharge of cold-start system at 2.75 MPa applied pressure.

The difference between these two curves can only be the sensible energy within the fuel system, remaining after the engine dynamometer test. While an exact thermal balance around the entire refueling process was not possible, the energy difference between the curves does correlate well with the total system heat capacity and temperature. In fact, it is possible to calculate that the cold-start modules were between 60 and 80°C at the start of the refueling test. The temperature of the modules was 77°C at the end of the engine dynamometer test, and some cooling must have occurred between the end of the engine test and the start of the refueling test (approximately 30 minutes). Of the total energy rejected by the modules, approximately 30% is due to sensible heat and 70% due to heat of reaction.

The cold-start module refueling tests can be summarized in Figures 17 and 18 which show the effect of coolant flow and applied hydrogen pressure on hydrogen recharge rate. Because not all refuelings involved a complete recharge of the cold start-modules, the measure of recharge rate (time to 90%), needs to be normalized to the mass of hydrogen absorbed. This produces a value of seconds/gram. The values shown in Figures 17 and 18 are simply the inverse of this mass normalized, time-to-90% computation.

The fact that increased hydrogen recharge pressure favors higher recharge rates is expected. This is because of the increase in the equilibrium reaction temperature of the hydride.

Since heat transfer rate is directly proportional to temperature difference, the recharge periods should correlate with equilibrium temperature, as below:

Applied Hydrogen Pressure, MPa	Equilibrium Temperature	ΔT to Coolant
2.75	46.0	40.0
2.40	42.6	36.0
2.07	37.7	31.3

Thus, the 2.75 MPa runs should be approximately 27% (40/31.3) faster than the 2.07 MPa recharge. The actual data show increases in recharge rates of between 19% (at high coolant flows) and 33% (at low coolant flows) by the increase in applied pressure.

The refueling rate is also coolant flow-limited, even with flows of 670 cc/sec (10.5 GPM). Unfortunately, the facility water supply system was incapable of higher delivered flows, so the effect of external heat transfer limits could not be eliminated during recharge tests.

MAIN BED REFUELING

As shown in Figure 19, the main bed refueling differs in many respects from the cold-start modules. First, the applied hydrogen

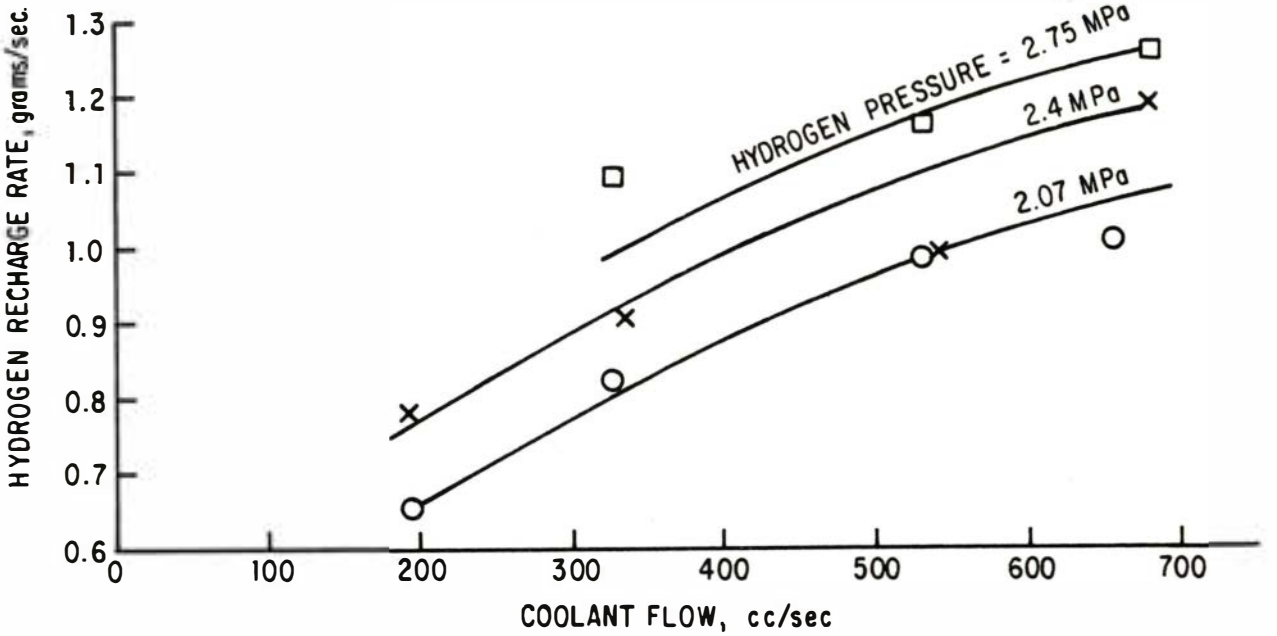

Figure 17. Hydrogen recharge rate for cold-start system as a function of coolant flow at 2.07, 2.4 and 2.75 MPa applied hydrogen pressure.

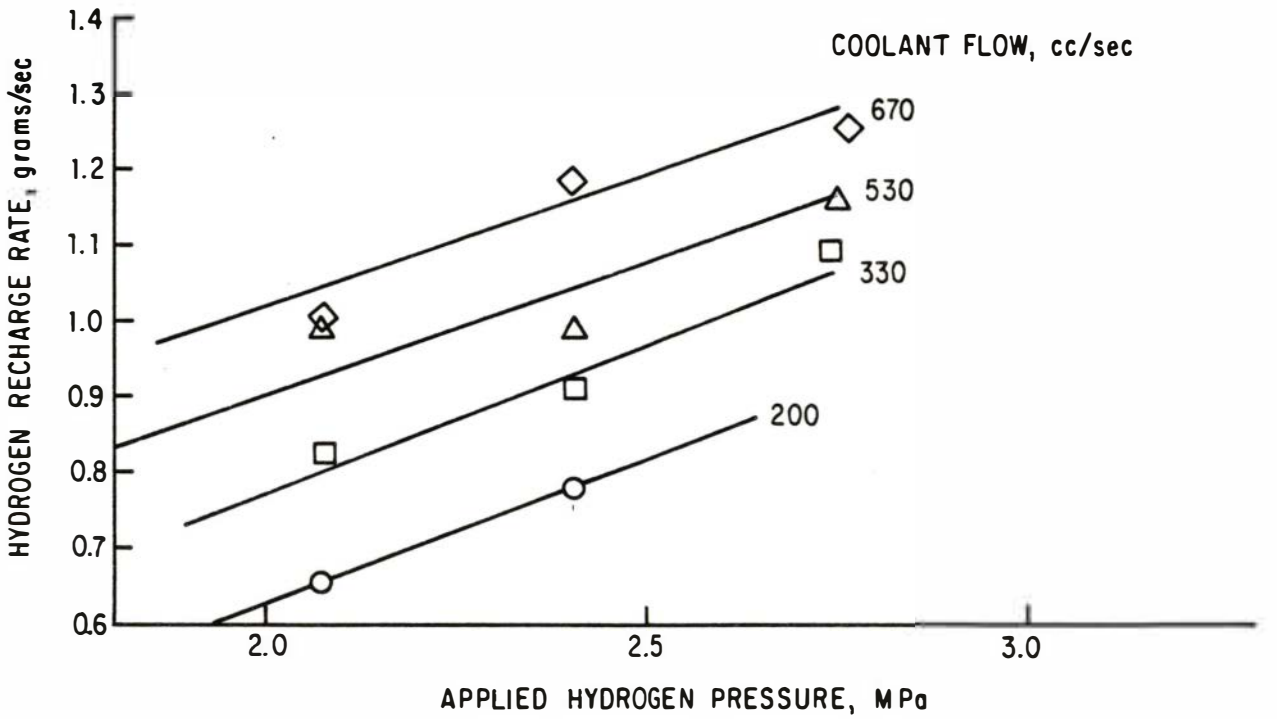

Figure 18. Hydrogen recharge rate for cold-start system as a function of applied hydrogen pressure at 200, 330, 530 and 670 cc/sec coolant flow.

pressure could not be maintained at the desired value (2.75 MPa) until nearly 850 seconds had elapsed. Note that the 90% recharge point occurs at approximately 940 seconds. Therefore, it would be more correct to classify this particular test as one in which the applied hydrogen pressure was closer to 2.5 MPa, not 2.75 MPa. The difficulty in maintaining the desired pressure is a result of the hydride recharge proceeding at a faster rate than the hydrogen supply regulator and plumbing can accommodate. Nearly all the main bed refueling exhibited slow bed pressure rises, but the short-fall was most pronounced at the higher pressure, higher coolant flow conditions.

During the first part of the refueling process in Figure 19, the hydrogen pressure is approximately 2.3 MPa. For the alloy in the main hydride beds, this pressure corresponds with an equilibrium temperature of 85°C. This is somewhat higher than the temperature of the fuel system immediately prior to the refuel test (approximately 79°C) which would tend to explain the steady rise and fall of the coolant outlet temperature in the first 60-120 seconds.

The difference between the "heat of reaction" and "heat rejected to coolant" curves in Figure 19 are worthy of a more detailed discussion than that presented for the cold-start modules. The total energy represented by the difference in these two curves cannot be explained by the sensible heat in the container metals and spent alloy or hydride alone. In order to produce a reasonable energy balance around the refueling process, the water contained within the modules at the start of the refueling tests must be included. While on the surface this appears logical, the inclusion of water mass in the energy balance implies that its mass is cooled continuously during the entire recharge. Apparently the coolant is not flowing through the main modules as slug-flow, but as a well mixed stream with eddys and backmixing.

Figures 20 and 21 show the effect of coolant flow and applied hydrogen pressure on recharge rate. As was shown for the cold start modules, higher recharge rates are favored by higher applied pressures and coolant flows.

The expected increase in recharge rate with applied hydrogen pressure (resulting from increases in the equilibrium temperature) is observed, but does not correlate well with the data. For example, the 2.75 MPa runs should be 14% faster than the 2.07 MPa runs, based on the temperature difference between the reacting hydride and the coolant. The actual data shows an increase of between 22 and 66%. On the other hand, the effect of raising the pressure from 2.40 MPa to 2.75 MPa should increase the recharge rate by some 6%. The actual data shows increases of between 3 and 10%. It is unclear as to why the higher pressure runs correlate well, but the 2.07 MPa recharge data does not.

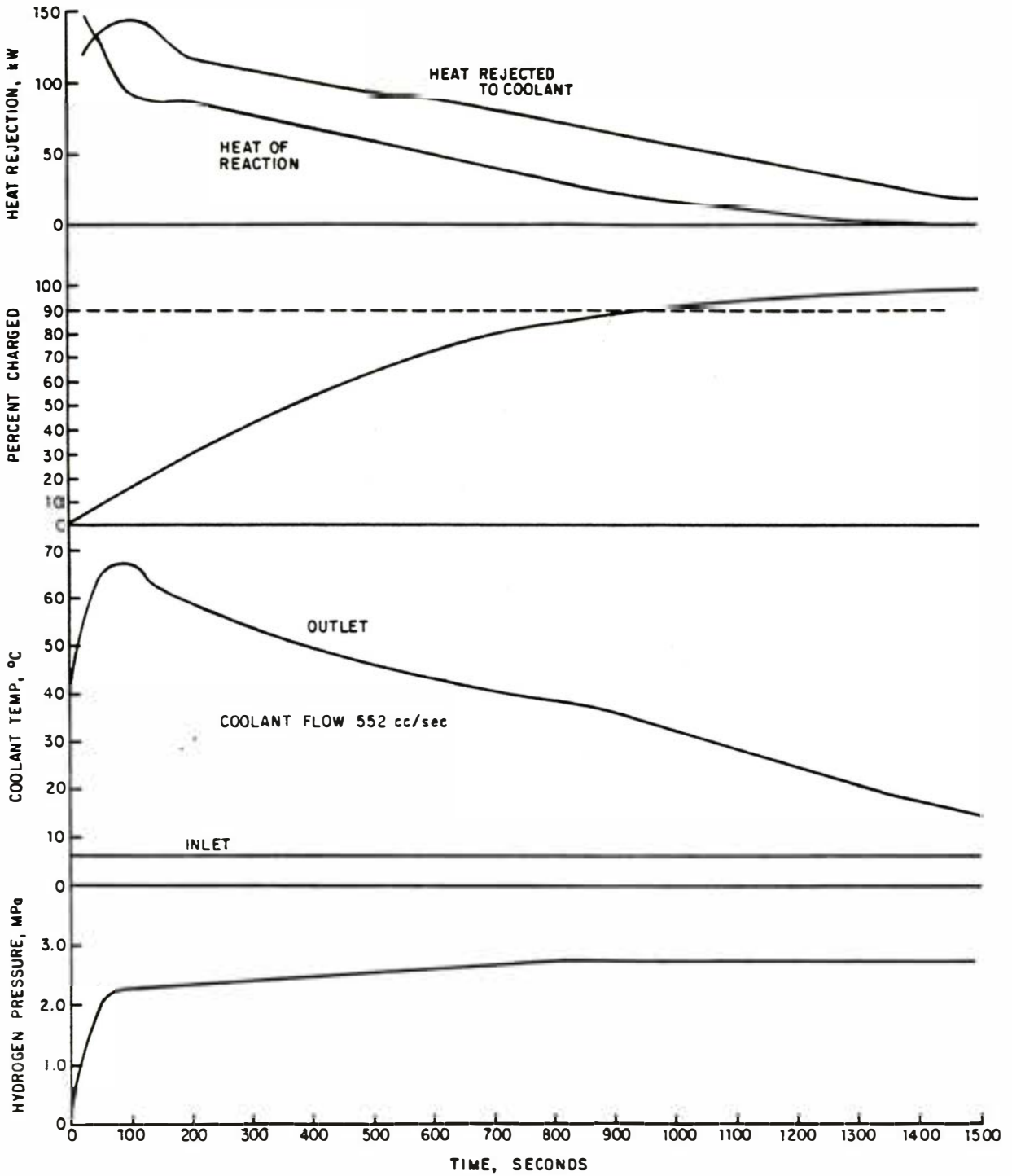

Figure 19. Hydrogen pressure, coolant temperature, fraction charged and heat flows during recharge of main fuel system at 2.75 MPa applied pressure.

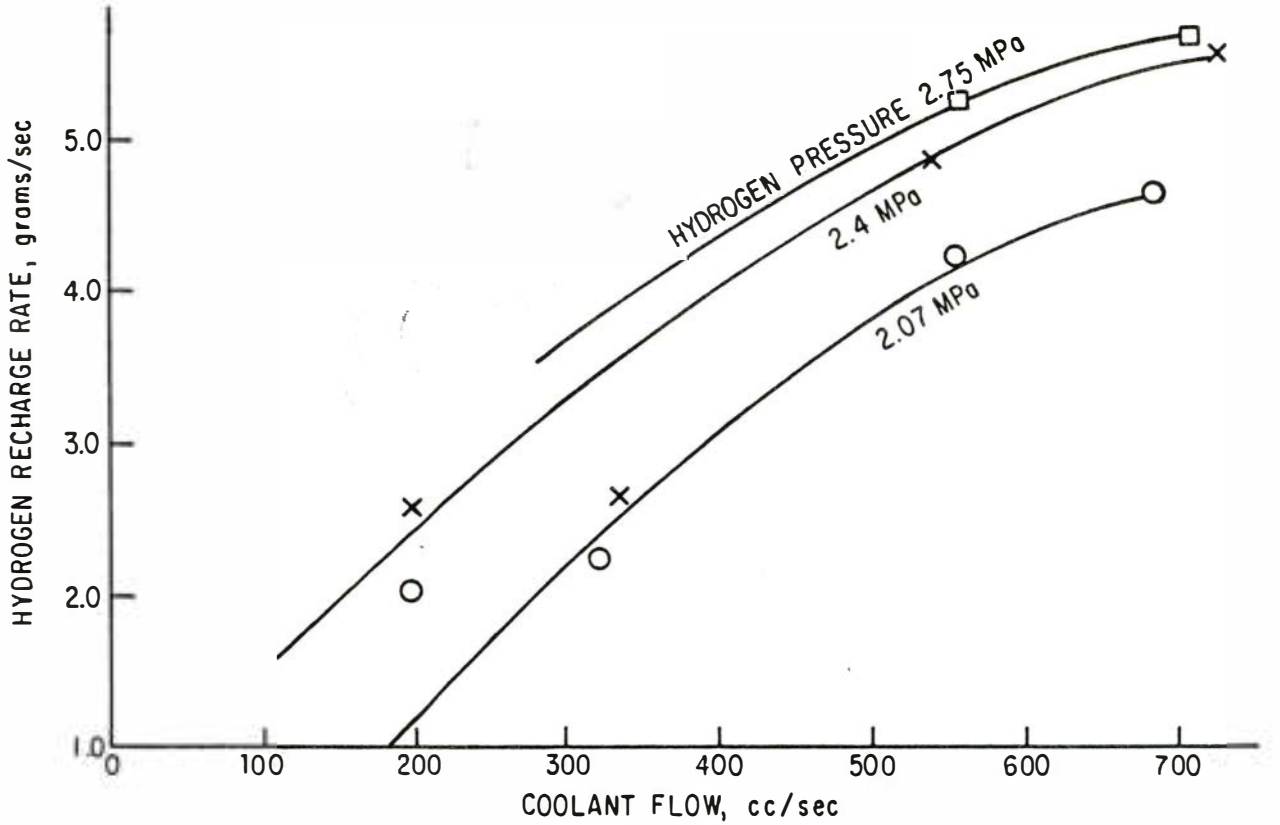

Figure 20. Hydrogen recharge rate for main fuel system as a function of coolant flow at 2.07, 2.4 and 2.75 MPa applied hydrogen pressure.

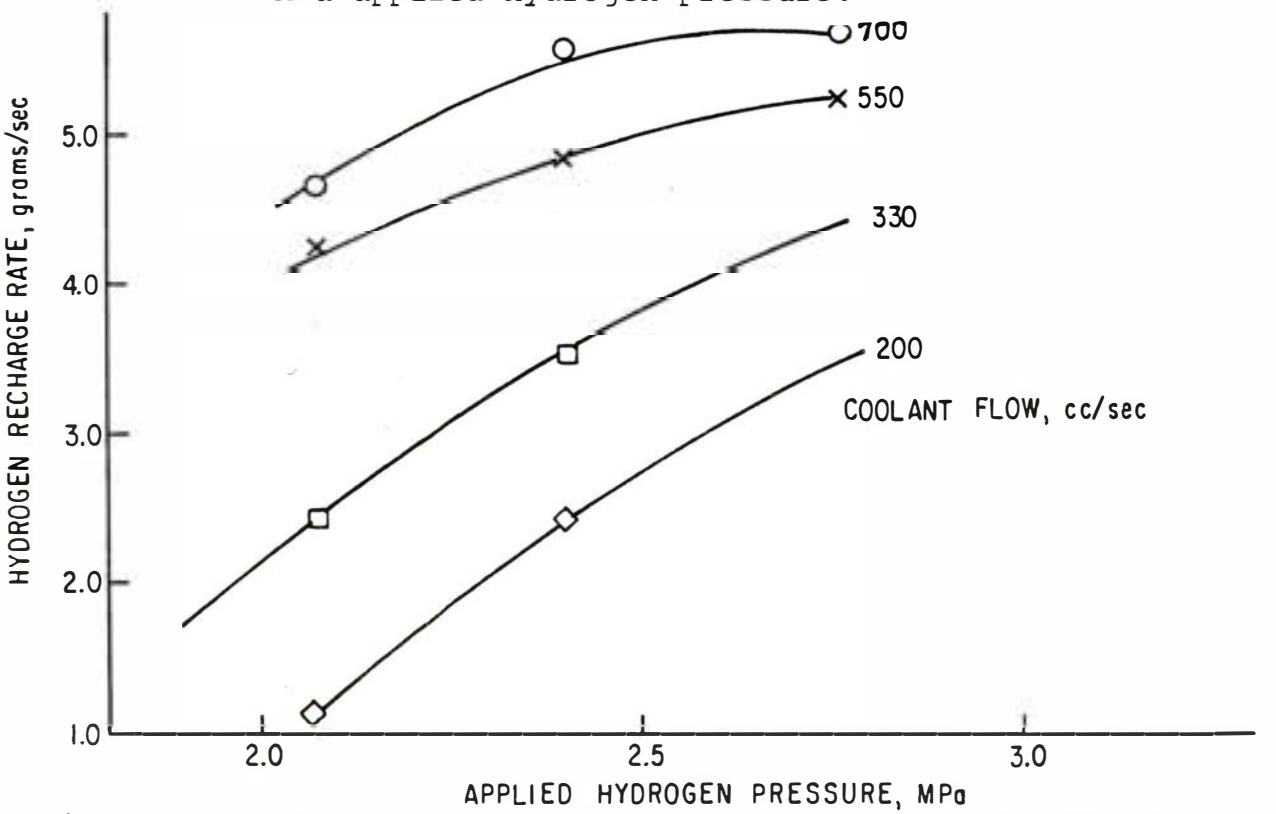

Figure 21. Hydrogen recharge rate for main fuel system as a function of applied hydrogen pressure at 200, 330, 550 and 700 cc/sec coolant flow.

VEHICLE REFUELING SIMULATION

On-board a mining vehicle, a metal hydride fuel system would be recharged in as simple an operation as possible, with no separate refuelings of cold-start and main bed modules. While the purpose of the current program phase was to gain information on module performance, one test was conducted with the hydrogen and coolant systems for the two hydride beds connected.

Referring back to Figure 10, it may be noted that both the cold-start and main beds can be fueled from a single quick-connect fitting, either QC1 or QC2, by opening valve V6. In addition, the coolant flows were connected in series by admitting tap water to QC4 on the cold-start bed and draining the main bed from QC3. The two fuel systems have a common connection (the normal drain manifold) which allows flow from the cold-start, through the main bed, and to drain.

The decision to flow the coldest water through the cold-start bed first was based on thermodynamic considerations. At the specified charging pressure of 2.75 MPa, the cold-start bed will have an equilibrium temperature of 46^{o}C, while the main bed will be at equilibrium at 88^{o}C. Therefore, the cold-start bed requires the coldest inlet water in order to even approach the high temperature differences which would be noted for the main bed. This is best illustrated in Figure 22. As shown in the Coolant Temperature curves, the cold-start bed, in the first several hundred seconds, operates at an average temperature of 10^{o}C.

The coolant exiting the cold-start bed is less than 15^{o}C for most of the refueling test, certainly sufficient to act as the heat sink for the main bed outlet.

With both hydride beds refueling simultaneously, the 90% recharge point occurred at 900 seconds (15 minutes). As might be expected, this is somewhat slower than the recharge period found for the main bed alone, under otherwise identical conditions of coolant flow and applied hydrogen pressure. It is however, much faster than the total time for charging the two systems consecutively.

CONCLUSIONS

All of the objectives of this phase of development have been met. The fuel system which was constructed supplies the 3304 Caterpillar engine with nearly 6 kg of hydrogen fuel at rates commensurate with the most demanding duty-cycles encountered by mining equipment.

The system far exceeds the goal of being able to start the engine at 4^{o}C (40^{o}F). It will deliver at least 3/4-power on a continuous basis starting from a cold condition. This would be adequate for most duty-cycles.

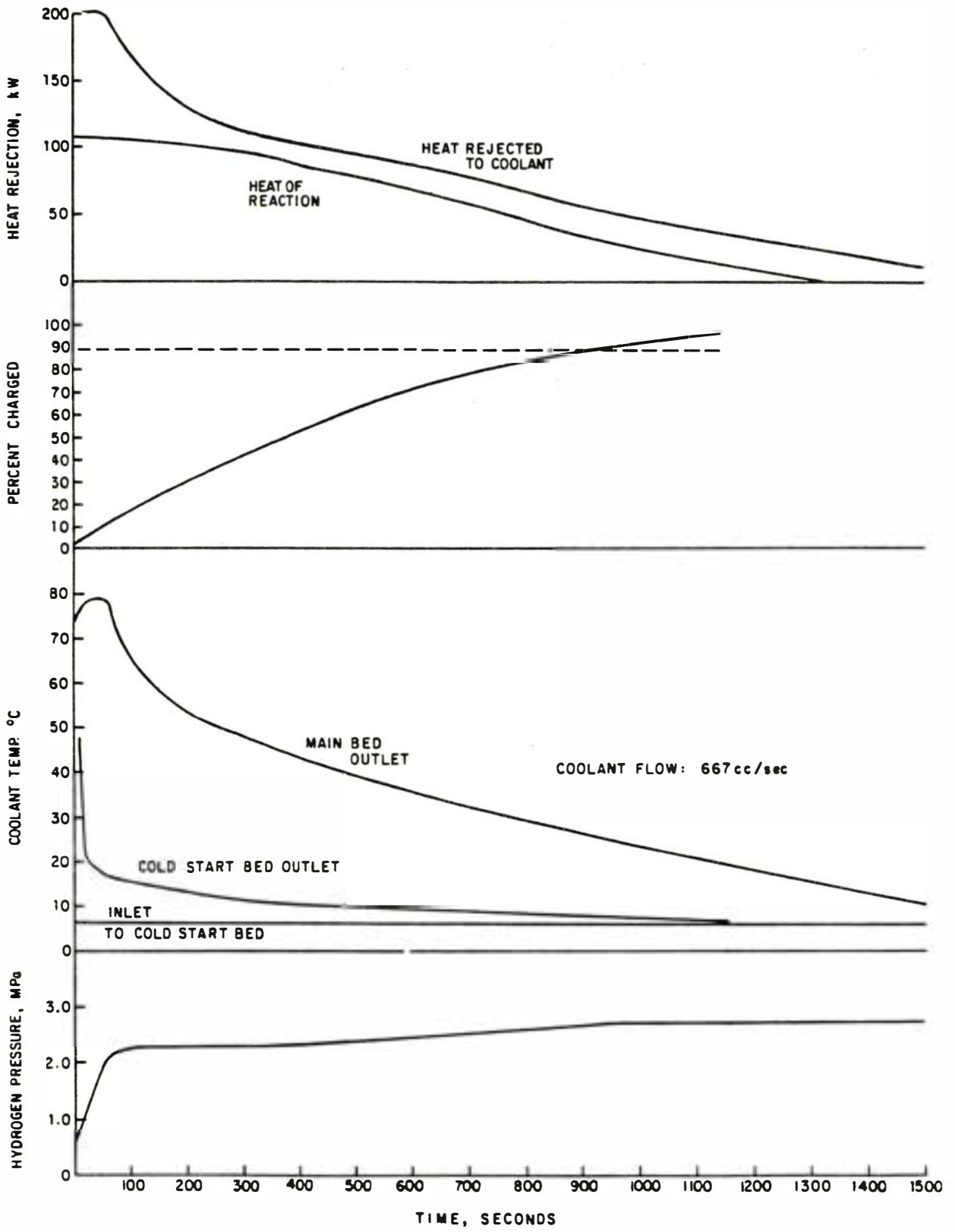

Figure 22. Hydrogen pressure, coolant temperature, fraction charged and heat flows during simultaneous recharge of both main and cold-start fuel systems.

The modular design of the system is a major advance over previous designs for a number of practical reasons and because it lends itself to the concept of a mine-safe, segmented hydride system. Mathematical modeling, bench-scale testing and the performance of a heat transfer enhanced prototype hydride module demonstrate that mine safety requirements can be met by dividing the fuel system into small, high-performance modules. One small module, when heated, can supply the engine's fuel demand but is not large enough to release a dangerous volume of H_2 in the event of an accident.

Refueling times vary with the hydrogen pressure used to charge the system and with the temperature and flow of coolant used during the process. Testing during this phase showed that the system can be 90% charged in 15 minutes with 2.75 MPa (387 psig) and 0.7 liters-per-second (10 gal/min) of cooling water at 6^{o}C (43^{o}F). The enhanced design will be capable of faster charging at lower temperatures.

The system, when supplemented with an additional 3 kg H_2-capacity hydride system during the next phase, will be ready for surface demonstration in a utility vehicle.

REFERENCES

1. N.R. Baker and F.E. Lynch, "A Hydrogen Engine Induction Technique for Backfire-free Operation", Final Report, Phase II U.S. Bureau of Mines Contract No. H0202034, May 30, 1982.

2. F.E. Lynch, "Ergenics Hydride Fuel System for a Caterpillar 3304 Hydrogen Engine", Final Report, Ergenics Division, MPD Technology Corporation, October 7, 1980.

3. F.E. Lynch, "Operating Characteristics of High Performance Commercial Metal Hydride Heat Exchangers",Proc. International Symposium on the Properties and Applications of Metal Hydrides", J. Less-Common Metals, 74 (1980) 411-418.

4. N.R. Baker, et al.,"A Clean Internal Combustion Engine for Underground Mining Machinery", Final Report, Phase I, U.S. Bureau of Mines Contract No. H0202034, December 31, 1981.

5. M. Ron, "Metal Hydrides of Improved Heat Transfer Characteristics", Proc. 11th Intersociety Energy Conversion Engineering Conference, State Line, Nevada, September 1976.

6. J.A. Jones,"$LaNi_5$ Hydride Cryogenic Refrigerator Test Results", Proc. 2nd Biennial Conference of Refrigeration for Cryogenic Sensors and Electronic Systems, December 1982

7. D.K. Edwards et al.,Transfer Processes, Holt, Rinehart and Winston, Inc., 1973

8. P.P. Turillon and G.D. Sandrock,"Hydrogen Storage Module", U.S. Patent #4,135,621, January 23, 1979.

9. N.R. Baker and F.E. Lynch, "Hydrogen Sorbent Flowaid Composition and Containment Thereof", U.S. Patent application, Ser. No. 400,440, July 21, 1982.

APPENDIX A

Construction and Performance of a Hydride Module with Enhanced Heat Transfer

As explained in the text of this report, mine-safe, ultra-low pressure fuel storage in metal hydride requires the development of hydride containers with enhanced heat transfer capabilities. This appendix will describe the construction of a full-scale, heat transfer enhanced hydride module which uses the bottle-brush method of increasing thermal conductivity in the hydride powders. The performance of this module during actual engine testing is also discussed.

The stainless steel heat exchanger used for this module is exactly the same as the 14 standard, capsule-type modules previously described and shown schematically in Figure 7. Instead of loading the heat exchanger tubes with hydride capsules however, a mixture of TFE powder (Ref.9) and hydride alloy powder was prepared and compacted amongst the copper bristles of cylindrical-shaped,"bottle"-type brushes. These brushes were inserted into the heat exchanger tubes, along with a tubular filter to carry hydrogen into and out of the powder. A cross-section of a tube is shown in Figure A-1.

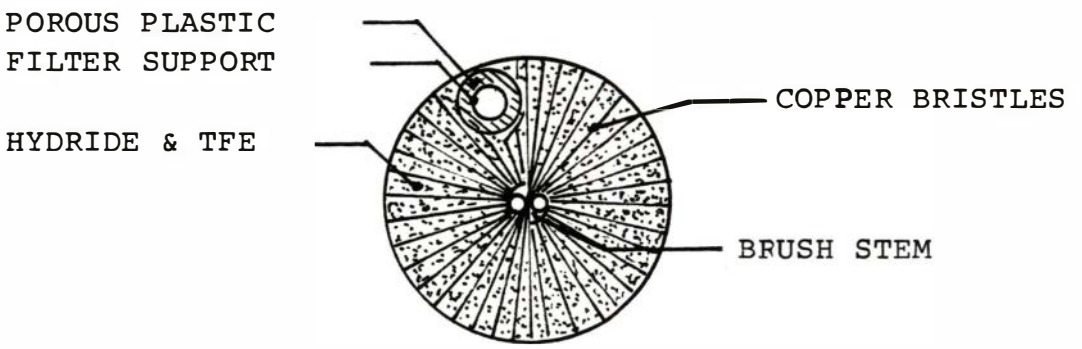

Figure A-1. Cross-section of a heat exchanger tube with bottle brush, flow-aid TFE powder and filter.

The specifications of the heat transfer enhanced module are listed in Table A. This table may be compared to Table 2 in the text of the preceding report. In doing so, it may be noted that the enhanced container holds less alloy (26.7 Kg vs. 33.9 Kg) due to the volume of the brushes and flow-aids. It is also less massive (53.4 Kg vs. 60.8 Kg) as a result of this reduced alloy capacity. The resulting hydrogen mass-percent calculated for the enhanced module is 10% less than the standard module.

The Cp ratio is 19% greater for the enhanced module than for the standard design. Cp ratio is an indicator of the dynamic response of a hydride system. Its effects are most important during cold-starting of the engine-hydride system and during rapid refueling of a hot hydride.

Table A. Specifications of the Heat Transfer Enhanced Hydride Module.

Type:	Tube and shell module with copper alloy brushes and TFE flow-aids.
Materials:	304 stainless steel container and filter support tube Chromium-copper alloy brush bristles Steel brush stems TFE flow-aid powder (3.5 micron) Poly propylene, pourous filter tubes
Construction:	All joints TIG-welded
Dimensions:	7 tubes-274 cm x 2.86 cm O.D. x 0.089 cm wall (108 in. x 1.125 in. O.D. x 0.035 in. wall) Shell O.D. - 8.89 cm (3.5 in.) Overall length - 277.2 cm (109.1 in.)

Effective external tube surface area: 1.7 M^2 (18.3 $ft.^2$)

Mass of Components:

Hydride Alloy	26.7 Kg	(58.6 lb.)
Container (including flow aid)	22.7 Kg	(49.95 lb.)
Liquid (as water)	3.7 Kg	(8.1 lb.)
Hydrogen Capacity	0.318 Kg	(.699 lb.)
Total Mass of Module	53.4 Kg	(117.5 lb.)

Calculated Hydrogen Mass-Percent: 0.60%

Table A. (Continued)

Hydride Alloy:	
Composition	$M^{*}Ni_{4.17}Fe_{0.83}$
Heat Treatment	None
25°C Nom. Desorp. Press.	10.3 Atm (154 psia)
Hysteresis Pressure Ratio	1.18
Heat of Reaction per g-mole H_2	6.3 Kcal
Heat Capacities:	
Hydride Alloy, charged	4.32 Kcal/°C
Hydride Alloy, discharged	2.35 Kcal/°C
Liquid (as water)	3.70 Kcal/°C
Container	2.98 Kcal/°C
Cp ratio $\frac{\text{Total Cp}}{\text{Hydride Cp}}$	= 2.55

* M denotes mischmetal, a group of rare-earth elements which occur naturally in ore.

The volume, mass and heat capacity penalties shown for the enhanced module are far outweighed by the performance gain.

The modeling experiments, reported in the text, showed a 370% improvement in heat transfer rate for the enhanced design compared to a standard, capsule-type system.

The full-scale, enhanced module was constructed and tested to verify that the changes in design could be scaled-up without difficulty. The enhanced module was found to be easier to fabricate and assemble than the older, capsule-type module because of the labor avoided by not making the aluminum capsules. The enhanced module passed the leak inspection with no problems and activated readily when exposed to hydrogen at 4.2 MPa (600 psig). Instead of repeating the charging tests performed on the bench-scale models, it was decided to make an operating comparison of the enhanced module vs. the standard module.

The comparison tests were conducted by cold-starting with a saturated hydride (2.5 MPa) at about 11°C (52°F) and holding the maximum possible load at 1200 RPM until each module was depleted. During these transient tests the engine was warmed from room temperature to 40-50°C (104-122°F) depending on the test duration.

The coolant control valve (PV2 in Figure 10) remained closed until the hydrogen pressure dropped below 1.2 MPa (160 psig). After the coolant control valve opened, 330 cc/sec (5.2 GPM) of engine coolant (water) began flowing through the test module.

The hydrogen pressure then continued to fall until full torque could no longer be maintained. It was after this occurred that the relative performance of the enhanced and standard modules could be compared. The engine torque leveled off at a value which indicated the specific power level which could be sustained by each module during this transient, cold-start test.

It was found that the standard module could sustain 0.42 kW per Kg of hydride alloy. The enhanced module could sustain 0.80 kW per Kg of alloy. This is considerably less than the projected 370% improvement but the difference can be reconciled.

Hydrogen Regulator restrictions cause a pressure drop which is directly related to flow. The higher flow at which the enhanced module was tested required 172 kPa gage (25 psig) upstream from the regulator to give the needed flow. At the lower power level, during the standard module test, only 83 kPa gage (12 psig) were required to produce the smaller fuel flow.

There was also a lack of comparability in the water temperature during the two tests. Since the lower power, standard module released its hydrogen more slowly, the engine had more time to gain heat. The mean water temperature during the comparison was 30°C for the enhanced module vs. 40°C for the standard module.

Despite this rough method of comparison, it is clear that the enhanced module can provide a high specific power. The utility vehicle, which the fuel system must serve, has a 75 kW engine and a 30% load factor. A continuous power requirement of 22.5 kW is indicated for the utility vehicle. At 0.80 kW per Kg of alloy, only 28 Kg are required in a module which can serve the engine's fuel demand. According to accidental fuel release calculations (Appendix B) which determines the maximum amount of hydrogen that can be accidentally released without creating an explosive mixture, a hydride module with up to 70 Kg of alloy is permissible.

APPENDIX B

Safety Analyses of Hydride Fuel Systems

This appendix examines some aspects in the use of hydride fuel systems for underground mining vehicles.

The degree of fuel hazard associated with the use of hydride fuel systems is not easily expressed in absolute terms. For that matter, complete safety cannot be attained in any "real-life" situation. As a concept, safety is a relative matter. But to come to terms with the safety aspect of hydrides used underground, an evaluation should be made of the amount of gas which a particular hydride system can release to the environment. Relative safety is then related to that gas volume and the hydride fuel system is designed accordingly.

Several safety criteria were examined in Reference 4, all of which were based on a control volume, whose size is determined by the dimensions of the smallest volume in which the particular vehicle may be found in the mining environment. The goal has been to set a "safe-release" limit for the hydride storage tanks, so that upon complete tank rupture, the concentration of hydrogen within the control volume is below the prescribed limit.

The amount of hydrogen released directly influences the magnitude of the potential damage. For high-pressure or liquid hydrogen storage methods, it is possible that all the fuel can be released instantly. The same is not true of hydrides. Hydrides can be designed to have a hydrogen pressure above, at, or below the atmospheric pressure. The safety advantage of this hydrogen storage method becomes apparent if one considers the inherent safety of a system employing a hydride with a hydrogen pressure at, or below atmospheric pressure. Should any part of the fuel system be ruptured, there is no driving force to cause hydrogen to evolve.

Determination of Safe Releases

Keeping in mind that a hydride storage system can limit the releasable amount of hydrogen, it is appropriate to ask how much hydrogen can be released and still be considered safe. While it may be tempting to place the answer at zero, it is unrealistic to require this of any fuel when analyzed under a "worst case" situation. As will be shown, the answer is not far removed from zero, and yet does allow for a reasonable fuel system design.

For this purpose, it is necessary to create a control volume. A natural one is an imaginary box representing the smallest volume in which a mining vehicle may be found.

This control volume was constructed as follows and is both conservative and restrictive:

- Length: Vehicle length + 2 ft each at front and rear
- Width: Vehicle width + 50%
- Height: Vehicle canopy height + 2 ft

The fuel system discussed in the present report was developed specifically for an EIMCO 975 Utility Vehicle. As specified above, the control volume for the 975 would be 61 m^3 (2160 ft^3). The "glass box" safety criterion proposed in Reference 4 allows fuel to be released into this control volume, as long as the overall concentration of fuel does not exceed 6% in air. Without violating this criterion, the fuel system could be ruptured and release up to 3.64 m^3 (129 scf) of hydrogen.

The fuel system envisioned for the EIMCO 975 will contain approximately 8 kg (97 m^3) of hydrogen. Because the above safety criterion will only permit the release of 3.64 m^3 of hydrogen, a constraint is thus placed on the fuel system design, allowing a release of only 3.8% (3.64/97.1) of the fuel content should the system be ruptured.

The basic equation governing what fraction of the stored hydrogen will be released is:

$$f_o = \frac{\bar{m}\,\overline{Cp}\,\Delta T}{n_{max}\,\Delta H} - k\left(\frac{P-1\ atm}{1\ atm}\right)$$

where:

f_o = fraction of the stored hydrogen released

$\bar{m}$ = average mass of the hydride and container

$\overline{Cp}$ = average heat capactiy of the hydride and container

ΔT = the difference between the temperature of the hydride and container at the time of the rupture and the temperature of the hydride when its hydrogen pressure is one atmosphere.

k = a constant dependent on the void spaces of the hydride and container

P = pressure of the hydride at the time of rupture

n_{max} = maximum number of moles of hydrogen stored by the hydride

ΔH = the heat of desorption necessary to release the hydrogen from the hydride

The first term is the ratio of the sensible heat of the system to the heat required to desorb the hydrogen. The thermal driving force for the desorption is the ΔT. The temperature of the hydride at the instant of rupture is determined by the design choices of the fuel system. At a minimum, this temperature must be sufficient to heat the hydride to produce the minimum fuel pressure required by the engine. The temperature of the hydride when its hydrogen pressure is one atmosphere is a property of the hydride itself. It should be understood that this will be the final temperature of the hydride and container shortly after rupture. At this point, the hydrogen pressure will be the same as the atmospheric pressure. Any further release of hydrogen is governed by the amount of heat which flows from the air surrounding the container, through the container's coolant and metals, through depleted alloy and into the hydrogen-containing hydride. Determining this subsequent leak rate is impossible without knowing the particulars of the hydride container design, but it should be insignificant compared to the initial release. Quantification of this subsequent leak rate is a subject of study in future phases of this program.

The equation which relates the temperature of the hydride when its pressure is one atmosphere (call it $T_{1\ atm}$) and its pressure, P, at any other temperature (T) is:

$$T_{1\ atm} = \left[\frac{1}{T} + \frac{R}{\Delta H} \ln \left(\frac{1\ atm}{P}\right)\right]^{-1}$$

The fuel system for the EIMCO 975 Utility Vehicle will contain two different hydride alloys. The cold-start system requires a hydride with useable pressures at 4°C (40°F). Therefore at a mine temperature of 25°C (77°F) its pressure will be much higher. A fuel system containing an unstable hydride will exhibit a high fraction of stored hydrogen releasable upon rupture. However, as will be demonstrated below, the heat transfer enhanced, cold-start unit with a high-pressure hydride can still meet the safety criterion.

The alloy used in the heat transfer-enhanced module had a 25°C pressure of 10.3 atm, and a heat of desorption of 6.3 kcal/mole of hydrogen.

Substituting these values into the above equation yields:

$$T_{1\ atm} = \left[\frac{1}{298^{\circ}K} + \frac{1.987\ cal/mol\text{-}^{\circ}K}{6300\ cal/mol} \ln \left(\frac{1\ atm}{10.3\ atm}\right)\right]^{-1}$$

$$= 244^{\circ}K, \quad -28.6^{\circ}C$$

In other words, the hydride temperature will fall to -28.6°C if its container is ruptured, while the internal gas pressure falls to one atmosphere.

The equation for fraction of stored hydrogen released may now be used, if the starting temperature and pressure are stated. In the following discussion, it is assumed that the heat transfer-enhanced, cold-start module is kept at 25°C by the engine coolant and that its pressure at time of rupture is 10.3 atmospheres. The basic equation is therefore (values are taken directly from Appendix A):

$$f_o = \frac{(11 \text{ kcal}/^oC)\ [25^oC - (-28.6^oC)]}{(318 \text{ gms } H_2)\ (\frac{1 \text{ mol}}{2.016 \text{ gms}})\ (\frac{6.3 \text{ kcal}}{\text{mol}})} + 0.001\ (\frac{9.3}{1})$$

$$= .596 + .0093$$

$$f_o = .605$$

It should be noted that this calculation is essentially independent of container size, since the ratio of $\bar{m}\ \bar{Cp}/n_{max}$ is constant for a given type of container and hydride alloy.

The heat transfer-enhanced module could supply hydrogen for a sustained engine load of 0.8 kW per kg of hydride alloy (See discussion of Appendix A). For the EIMCO 975 Utility Vehicle, the average engine load is projected to be 22.5 kW (30% assumed load factor, 75 kW engine). This engine load could be sustained with a single, heat transfer-enhanced module with a hydride alloy mass of 28 kg (22.5 kW ÷ 0.8 kW/kg of alloy). The amount of hydrogen contained by the 28 kg of alloy would be 0.33 kg (140 scf).

If this single, heat transfer-enhanced module were ruptured, the fraction of fuel released (as calculated above) would be 60.5% of 0.33 kg, or 0.2 kg (85 scf). This release of fuel would be considered "safe" under the "glass box" control volume criterion, which would allow the release of up to 0.305 kg (129 scf).

The main hydride system for a mine-safe vehicle requires a slightly different approach to meeting the safety criterion. Because it contains the majority of the 8 kg of stored hydrogen, the fraction releasable is at least an order of magnitude less than the cold-start system.

In order to meet the safety criterion, the hydride alloy in the main system will need to be a very low pressure composition. However, the hydrogen pressure required by the engine fuel control system drives the design towards higher pressures than those safely permitted. One possible solution to this dilemma is the use of small hydride containers, sequentially heated so as to produce engine-usable pressures. The heat transfer-enhanced design of Appendix A allows the use of small, high-performance hydride modules. These units could utilize hydride alloys with atmospheric or sub-atmospheric hydrogen pressures at ambient temperatures. As needed, individual modules would be heated to temperatures near the engine coolant temperature, in order to produce the fuel pressure

required by the engine fuel control regulators, and fuel line pressure drops. If one of these modules is ruptured in the heated state, the fraction released will be important, while the fuel depleted units and the yet-to-be-used modules will not be able to release hydrogen.

During the next project phase, several of these stable hydride modules will be constructed and, using the methods of this appendix, the hydrogen release potential will be calculated.